eng

MDPI

Article

Integrated Multi-Parameter Experimental Assessment of Cylinder-Bore Geometry, Surface Integrity, and Sealing-Related Indicators in ICE and HEV Engines Under Controlled Dynamometer Operation

Muhammad Amir Sabrin Aznan [1], Mohamed Thariq Hameed Sultan [1,2,3,*], Jan Lean Tai [1] and Navaneetha Krishna Chandran [2]

[1] Department of Aerospace Engineering, Faculty of Engineering, Universiti Putra Malaysia, Serdang 43400, Selangor, Malaysia; gs75369@student.upm.edu.my (M.A.S.A.); taijanlean2008@hotmail.com (J.L.T.)
[2] Laboratory of Biocomposite Technology, Institute of Tropical Forest and Forest Product (INTROP), Universiti Putra Malaysia, Serdang 43400, Selangor, Malaysia; navaneetha@upm.edu.my
[3] Aerospace Malaysia Innovation Centre [944751-A], Prime Minister's Department, MIGHT Partnership Hub, Jalan Impact, Cyberjaya 63600, Selangor, Malaysia
* Correspondence: thariq@upm.edu.my

Abstract

This study integrated quality-inspection records, bore measurements, and dynamometer data to assess cylinder-bore geometry, surface integrity, and engine-level blow-by and oil consumption in internal combustion (ICE) and hybrid electric vehicle (HEV) engines. Six four-cylinder engines (three per group) were selected through quality-control sampling. Initial measurements were taken after machining and before assembly; post-test measurements followed engine assembly, dynamometer testing at 6000 rpm and 100% torque, and dismantling. Bore geometry was measured using a dial bore gauge, roundness measurement system, and coordinate measuring machine; surface condition was assessed by stylus profilometry and replica-based cross-hatch microscopy. ICE engines showed larger increases in diameter and ovality, whereas HEV engines showed larger increases in roundness and cylindricity. Ra decreased by 0.048 µm for ICE and 0.008 µm for HEV, while cross-hatch evaluations remained acceptable. Mean blow-by and oil consumption were lower for HEV (18.20 L/min and 8.75 g/h) than for ICE (19.62 L/min and 10.76 g/h); all engines met the acceptance limits. Exploratory analysis indicated stronger associations of roughness changes with blow-by and oil consumption than geometric parameters. The findings provide an integrated assessment but are limited to six engines under a full-load condition; assembly, thermal exposure, and wear effects could not be isolated.

Keywords: cylinder-bore deformation; cylinder liner; surface roughness; cross-hatch; blow-by; oil consumption; internal combustion engine; hybrid electric vehicle

Check for updates

Received: 12 October 2026
Revised: 1 November 2026
Accepted: 20 November 2026
Published: 27 November 2026

Copyright: © 2026 by the authors. Licensee MDPI, Basel, Switzerland. This article is an open access article distributed under the terms and conditions of the Creative Commons Attribution (CC BY) license.

1. Introduction

1.1. Cylinder Bore Deformation and Engine Performance

The cylinder bore is one of the most functionally important surfaces in a reciprocating internal combustion engine because it provides the running surface for the piston and ring pack while contributing directly to gas sealing and oil control. The interaction between the piston rings and the liner is governed by bore geometry, surface texture, lubrication, ring

motion, and operating conditions. Consequently, even small changes in the bore condition can influence ring conformity and the resulting tribological response [1,2].

Cylinder bore deformation does not occur through a single mechanism. The bore is subjected to assembly loads before engine operation and subsequently experiences thermal and mechanical loadings during operation. Head-bolt preload, gasket compression, combustion pressure, piston-side thrust, temperature gradients, and structural constraints can produce dimensional and form changes along the bore. Previous investigations have demonstrated that cylinder-liner deformation can influence ring-pack sealing and friction power, indicating that bore geometry is relevant not only as a dimensional characteristic but also as part of the functional ring–liner system [2]. Three-dimensional modelling of the piston ring–bore contact has similarly demonstrated that the local bore geometry affects the distribution of ring contact and separation during engine operation [3].

The resulting deformation may appear in several forms. A change in the overall bore size can be represented by diameter variation, whereas directional distortion can be reflected through ovality and roundness. Axial changes can produce taper, whereas three-dimensional form errors may be described using cylindricity. Straightness and bore-position measurements provide additional information when the bore axis itself is displaced or distorted. Previous dimensional studies have shown that these characteristics can vary along the bore and should therefore not be assumed to remain uniform over the complete cylinder length [4].

Therefore, bore deformation should be interpreted using a combination of geometric indicators rather than a single-dimensional measurement. A diameter value alone may identify a change in bore size but cannot distinguish whether the change is uniform, directional, localised, or distributed along the bore. Therefore, multi-parameter assessment is particularly important when dimensional changes are subsequently related to sealing-related measurements.

1.2. Bore Surface Integrity and Sealing-Related Behaviour

Bore geometry provides only one part of the functional condition of a cylinder. The honed liner surface forms the immediate interface with the piston-ring pack, and its texture influences lubricant distribution, ring interaction, friction, running-in, and wear. Reviews of plateau-honed cylinder-liner surfaces have highlighted the importance of considering several surface parameters together because no single roughness parameter can fully describe the functional texture of a honed bore [5]. Surface-texture studies have similarly shown that groove characteristics influence lubricant transport and the tribological behaviour of the ring–liner interface [6–8].

Cross-hatch geometry is particularly important because the intersecting honing grooves provide pathways associated with lubricant distribution and retention. The cross-hatch angle can influence the ring–liner interaction and tribological behaviour, although its effect depends on the surrounding groove and surface characteristics rather than the angle alone [9]. Experimental investigations have also demonstrated that changes in honing processes and surface texture can modify the resulting cylinder-liner surface condition [5,6].

However, in practical engine inspections, surface acceptance is often based on defined inspection criteria, such as cross-hatch regularity, honing width, burr or kaeri condition, and porosity. These criteria are useful for identifying gross surface defects, but may not fully capture smaller changes in roughness or bore geometry occurring during engine operation. Consequently, combining numerical surface parameters with microscopic surface inspection provides a more complete description of the post-test condition.

The relationship with sealing-related behaviours must also be treated carefully. Blow-by gas represents leakage from the combustion chamber to the crankcase through the ring

pack and, therefore, reflects the behaviour of the complete sealing system rather than the bore surface alone [10]. Ring mobility, ring gap, combustion pressure, bore geometry, and operating speed can influence gas leakage [3,10]. Similarly, oil consumption is a multifactorial response involving the ring pack, oil film behaviour, evaporation, drain-back, crankcase ventilation, and other engine components [11]. Therefore, blow-by and oil consumption should be interpreted as supporting engine-level indicators when evaluating the bore and surface conditions, rather than as direct measurements of bore deformation.

1.3. Research Gap and Objective

The literature contains substantial studies on cylinder-liner deformation, surface texture, piston ring interaction, and sealing behaviour. However, these aspects are frequently investigated separately. Bore geometry is commonly evaluated through dimensional or form measurements, whereas surface studies focus on roughness and honing characteristics, and engine studies often report blow-by or oil consumption as performance indicators [2,5,10,11]. This separation makes it difficult to determine how measurable post-test changes in the bore condition are reflected across different levels of the engine system.

A further limitation concerns the interpretation of acceptable surface condition. A bore may satisfy conventional cross-hatch inspection criteria while still experiencing measurable changes in surface roughness or geometric form. Surface texturing studies indicate that the functional state of a honed liner depends on characteristics beyond simple visual confirmation of a cross-hatched pattern [6,9]. Therefore, an integrated experimental assessment is needed to examine bore geometry, surface roughness, cross-hatch condition, and sealing-related engine responses under the same controlled operating exposure.

To address this gap, this study brings together measurements already collected at different stages of the production and testing processes. Bore geometry, surface roughness, cross-hatch condition, and bore position were recorded during routine weekly quality inspections, whereas blow-by and oil consumption were obtained during dynamometer testing. Six-cylinder blocks comprising three ICE and three HEV units were selected during routine inspection and traced through production and engine assembly to their corresponding dynamometer tests. This allowed the initial inspection data to be compared with post-test bore measurements and engine-level responses. Therefore, this study examines how these existing measurements can be interpreted together within a consistent pre-test and post-test framework without introducing new measurement equipment or replacing established inspection procedures. The following research question guided this study:

How do cylinder bore geometry and surface-integrity characteristics change following controlled dynamometer operation, and how are these changes associated with blow-by and oil-consumption responses in ICE and HEV engines?

Accordingly, the objective of this study is to experimentally assess the changes in cylinder-bore geometry and surface integrity and examine their relationship with sealing-related indicators, namely, blow-by gas and oil consumption, for ICE and HEV engines under controlled dynamometer operation.

This study does not attempt to establish a single causal mechanism between any individual bore parameter and engine-level response. Instead, geometry, surface texture, cross-hatch condition, blow-by, and oil consumption are interpreted as a connected set of measurements that provide a broader picture of the post-test cylinder-bore condition.

2. Materials and Methods

2.1. Experimental Design and Engine Samples

An experimental before-and-after design was adopted to evaluate the changes in the cylinder-bore geometry, surface integrity, and sealing-related indicators following controlled

dynamometer operation. Six new production engines were included, comprising three ICE and three HEV units. The corresponding cylinder blocks were selected through routine weekly quality control sampling, with each block sampled during the same production week in which it was machined. Following routine cylinder-bore inspection, the selected blocks were traced through the normal production and engine assembly processes before being sent for dynamometer testing. Each engine contained four cylinders, providing 24 cylinder-level measurement units for geometric and surface investigations. Engine identifiers were retained to maintain traceability between the initial block inspection, subsequent assembly, and dynamometer results.

For confidentiality reasons, the vehicle model names and engine identification codes were not disclosed. This study compared a conventional 1.5 L (1496 cc) ICE configuration with a 1.5 L hybrid electric vehicle (HEV) configuration. Both combustion engines have four cylinders and use a DOHC arrangement with Dual VVT-i. The HEV configuration also includes an electric motor and a hybrid battery as part of the powertrain.

The comparison was based on specifications relevant to cylinder-bore geometry and surface condition. According to the applicable part drawings, both configurations had the same nominal bore diameter of 72.5 mm, bore height of 130 mm, cylinder-block material (ADC12 with T5 heat treatment), and cylinder-liner material (FC230). Both engine groups underwent the same general production and assembly procedures and were evaluated using the same dynamometer procedure. The principal comparison was conducted at 6000 rpm and 100% torque.

Despite these common characteristics, the two engine configurations were not identical. The HEV operated with electric motor assistance, whereas the cylinder-block designs differed, including the provision for starter attachment in the ICE configuration. The coolant temperature monitoring location also differed between the groups: around the TCC area for the ICE and on the exhaust side, closer to the water jacket and cylinder-bore area, for the HEV. The engines originated from different production dates and batches, although no abnormal production, assembly conditions, or rework were reported. These structural and production-related differences may have influenced their measured responses. Therefore, the findings are limited to the six tested engines and should not be interpreted as establishing a general equivalence between ICE and HEV configurations.

The two measurement stages were linked to the production and dynamometer sequence. M1 was obtained during routine weekly quality-control inspection after machining and before engine assembly. Following engine assembly and dynamometer testing, the engine was dismantled in stages, with component-related checks, including leak and torque-value checks, carried out during the process until only the cylinder block remained for post-test measurement (M2). Before M2, the cylinder block was allowed to cool; however, no fixed cooling duration was specified. The cylinder bore interior was cleaned using FT Jumbo Cleaner spray (Market Asia Co., Plaeng Yao, Chachoengsao, Thailand) and wiped until clean before measurement. The same measurement positions and general measurement setup were used for M1 and M2 to support direct comparison.

Cylinder-bore measurements were performed at predefined axial locations to capture the variation in bore condition along the cylinder length. Multi-region measurements are important because bore deformation can vary with axial position owing to differences in thermal exposure, mechanical loading, structural constraint, and piston-ring interaction [12,13]. Similarly, surface measurements were registered at fixed axial locations so that changes in roughness and surface texture could be evaluated consistently before and after engine operation. The experimental design is summarised in Table 1.

Table 1. Experimental design, instrumentation, and principal measurement settings.

Domain	Instrument/Arrangement	Key Settings/Outputs
Study design	3 ICE and 3 HEV engines; 4 cylinders per engine	M1 (pre-test) and M2 (post-test)
Dynamometer condition	Controlled engine-dynamometer test (Meidensha Corporation, Tokyo, Japan; Model EB-ANR)	6000 rpm; 100% torque (full load)
Bore diameter/ovality/ taper	Peacock No. 5 dial bore gauge (Ozaki Mfg. Co., Ltd., Tokyo, Japan)	Resolution 0.001 mm; 10, 60, 115 mm; X/Y directions
Roundness/form	Roncorder EC4100/EC5100 series (Kosaka Laboratory Ltd., Tokyo, Japan); MC-92112 PU-UD3 stylus	Measurements at predefined axial positions
Bore position/datum geometry	Mitutoyo Crysta-Apex S CMM (Mitutoyo Corporation, Kawasaki, Japan); Renishaw SCR200 probe (Renishaw plc, Wotton-under-Edge, UK)	Fixed engine reference system
Surface roughness	Mitutoyo Surftest SV-3100 (Mitutoyo Corporation, Kawasaki, Japan)	Ra, Rz, Rk, Rpk, Rvk, Mr1, Mr2; 10, 60, 115 mm
Cross-hatch surface	Replica film (LADD Research Industries, Essex Junction, VT, USA) + Nikon SMZ1270 stereomicroscope (Nikon Corporation, Tokyo, Japan)	Middle/front region; nominal 8×; six image locations per replica
Cross-hatch criteria	Microscopic inspection	Angle 30° ± 2°; line/burr score ≥ 3; honing width ≤ 30 µm
Engine-level indicators	Dynamometer-facility measurements	Blow-by gas and oil consumption; compression and thermal values as supporting controls

The overall experimental workflow consisted of baseline dimensional and surface measurements, controlled engine operation on the dynamometer, post-test measurements, and integration of cylinder-level and engine-level responses. The resulting framework was designed to distinguish direct condition measurements from broader engine-level response indicators.

2.2. Cylinder-Bore Geometry and Dimensional Characterisation

Cylinder-bore geometry was characterised using complementary dimensional and form-measurement techniques. A dial bore gauge was used for bore-diameter measurements, while a coordinate measuring machine (CMM) and a roundness measurement system were used for form and positional characteristics. The combination of these techniques enabled the assessment of both local dimensional changes and broader geometrical deformation.

A Peacock No. 5 mechanical dial bore gauge was used for manual bore-diameter measurements. It was selected because it is the standard instrument used for routine bore-diameter inspection at the DPEM. The gauge has a resolution of 0.001 mm, allowing readings to be recorded to three decimal places, consistent with the decimal precision used in the applicable bore specification. Before measurement, the gauge was zero-set using a setting bar in accordance with the established standard operating procedure (SOP). Measurements were taken at three predefined axial positions (10, 60, and 115 mm from the deck surface) in two orthogonal directions (X and Y). Three readings were taken at each measurement point, and their arithmetic mean was used as the recorded value. The same measurement

locations and reference directions were maintained between the pre-test (M1) and post-test (M2) stages.

The CMM measurements were performed using a Mitutoyo Crysta-Apex S coordinate measuring machine equipped with a Renishaw SCR200 probe system. The CMM was primarily used for bore position and related datum-based measurements. The bore position was evaluated in the defined upper and lower measurement regions using the established engine reference system. The use of a fixed datum is important because bore position and axis-related measurements are highly sensitive to the coordinate system definition and workpiece setup [13].

The Roncorder EC4100/EC5100 series form-measurement system equipped with an MC-92112 PU-UD3 stylus was used to measure roundness, cylindricity, parallelism, and straightness. Roundness was evaluated at predefined axial positions, while parallelism and straightness were measured over the defined bore length using the established front–rear and intake–exhaust reference directions. The same predefined measurement locations and workpiece orientation were maintained between M1 and M2.

The selected measurement characteristics represent different aspects of the bore condition. The diameter describes the overall bore size, ovality represents directional diameter variation, taper describes axial dimensional variation, roundness characterises the cross-sectional form, and cylindricity considers the three-dimensional cylindrical form. Straightness and bore position provide additional information regarding bore-axis alignment. Such complementary measurement strategies are useful because a single bore-diameter measurement cannot distinguish between uniform dimensional change and directional or localised distortion [4,12,13]. The dial bore gauge zero-setting arrangement and bore-diameter measurement are shown in Figure 1a,b, while the CMM and roundness measurement system are shown in Figure 1c,d.

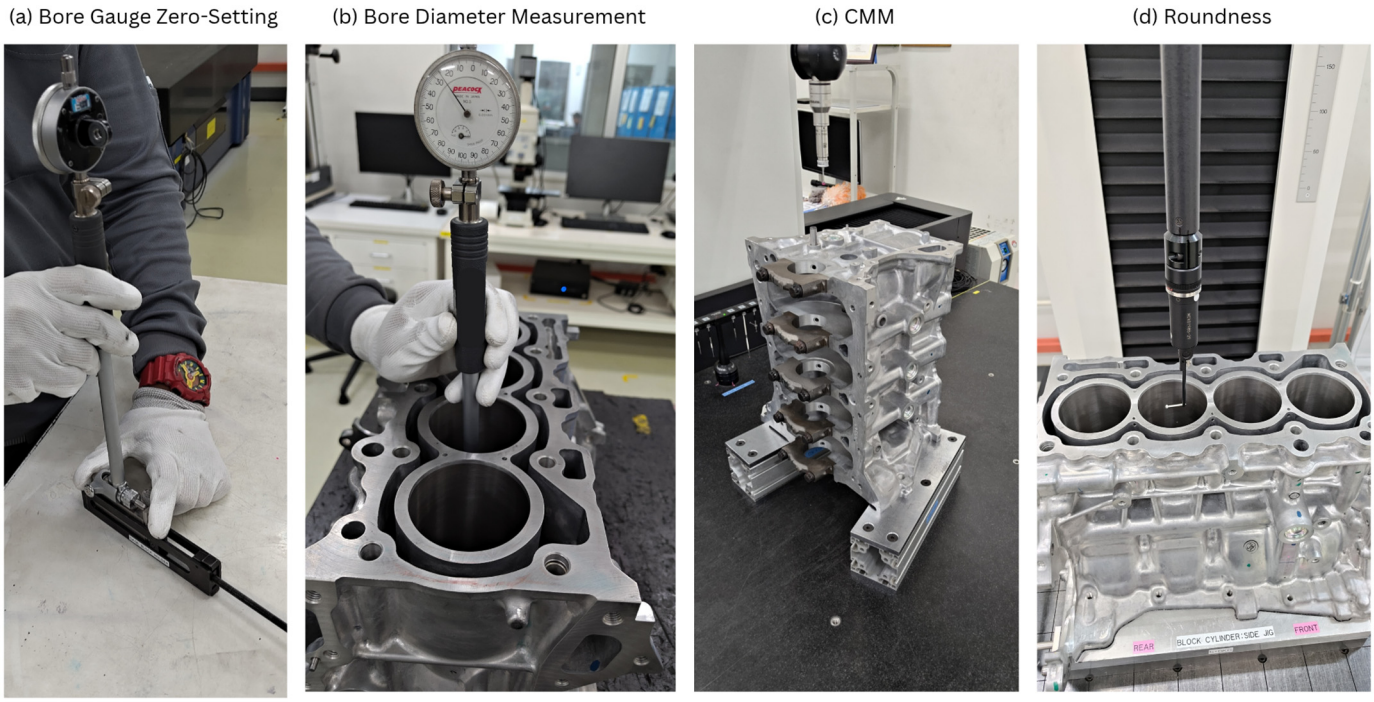

Figure 1. Measurement systems used for cylinder-bore geometric characterisation: (**a**) zero-setting of the Peacock No. 5 dial bore gauge using a setting bar in accordance with the established SOP; (**b**) manual bore-diameter measurement at the predefined axial positions and in two orthogonal directions; (**c**) coordinate measuring machine (CMM) used for datum-based bore-position measurements; and (**d**) roundness measurement system used for circumferential form measurements.

For the before-and-after comparison, the dimensional change in each parameter was calculated as follows:

$$\Delta X = X_{M2} - X_{M1} \quad (1)$$

where X_{M1} represents the measured value before dynamometer operation and X_{M2} represents the corresponding post-test value. Positive and negative values were retained to preserve the direction of dimensional change.

For taper, both the magnitude and directional interpretations were considered according to the predefined measurement convention. Ovality was obtained from the difference between the orthogonal X and Y diameter measurements. Multi-region measurements were retained throughout the analysis because axial variation is an important characteristic of bore deformation and cannot be identified reliably from a single measurement height [12,13].

2.3. Surface Roughness and Surface-Texture Characterisation

The cylinder-bore surface roughness was measured using a Mitutoyo Surftest SV-3100 stylus-based surface profilometer. Measurements were obtained at three axial positions corresponding to 10 mm (top), 60 mm (middle), and 115 mm (bottom) from the deck surface. The measurement was performed on the front side of each cylinder, with the stylus traced from bottom to top.

The roughness parameters evaluated were Ra, Rz, Rk, Rpk, Rvk, Mr1, and Mr2. Ra and Rz were retained as general amplitude descriptors, whereas Rk, Rpk, and Rvk were used to describe the core, peak, and valley characteristics of the surface profile. Mr1 and Mr2 were included to describe the material ratio characteristics of the measured profile.

Only one roughness trace was recorded at each predefined location for each measurement stage. Accordingly, the individual roughness traces were treated as measurement observations rather than repeated replicate measurements. This distinction is important because repeated observations should not be implied where they were not performed. Therefore, the measurements represent local surface observations, and local variations in the honing texture cannot be completely separated from the measured changes.

The bore surface was cleaned before roughness measurement using the designated cleaning procedure to minimise the influence of oil, debris, or loose surface contamination. The same axial locations, circumferential orientation, measurement direction, and measurement procedure were maintained between M1 and M2.

The selection of multiple roughness parameters was based on the recognised limitation of using Ra alone to describe a functional honed surface. Plateau-honed cylinder liners contain peaks, core regions, and valleys with different functional roles, particularly in relation to running-in and lubricant retention [5,14,15]. Surface texture and groove characteristics may also influence lubricant transport and the tribological response of the piston ring/liner pair [6,16,17]. The stylus measurement arrangement and microscopic surface evaluation are shown in Figure 2.

For each roughness parameter, the before-and-after change was calculated as

$$\Delta R = R_{M2} - R_{M1} \quad (2)$$

where R represents the corresponding surface parameter.

Because the bore surface is anisotropic and contains an intentionally generated honing texture, changes in roughness parameters were interpreted together with cross-hatch observations rather than as isolated indicators of surface degradation. The surface characterisation methodology and profile evaluation can also be affected by filtering and processing conditions, making consistent measurement settings important for comparative studies [18–20].

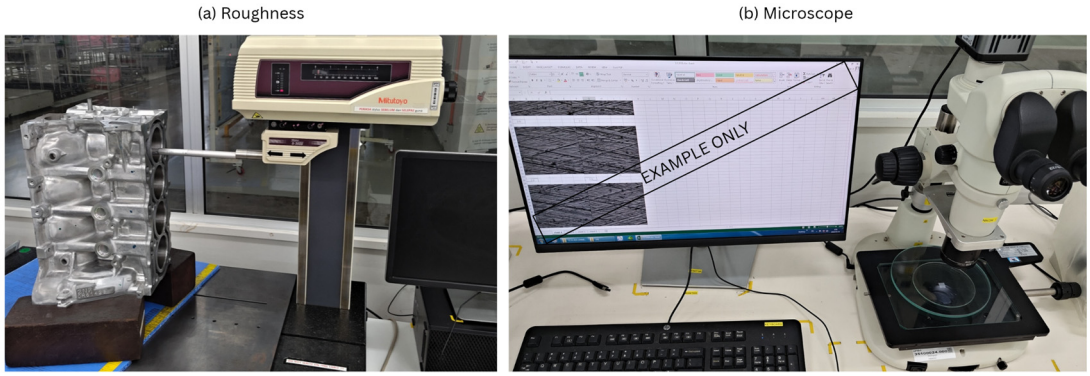

Figure 2. Cylinder-bore surface-texture characterisation: (**a**) stylus-based roughness measurement at the predefined axial locations on the front side of the bore, with the tracing direction maintained from bottom to top; and (**b**) microscopic evaluation of the measured surface texture for qualitative confirmation of the honed-surface condition.

2.4. Cross-Hatch Replication and Microscopic Evaluation

The crosshatch condition was evaluated using a replica-based microscopic method. Before replication, the cylinder bore was cleaned to remove loose contaminants and residual lubricant. A small piece of replica film, approximately 10 mm × 20 mm in size, was prepared for each evaluation location. Ethyl acetate with a minimum purity of 99.8% (Acros Organics BVBA, Geel, Belgium) was applied between the bore surface and replica material to promote conformal contact with the honed texture.

The replica was gently pressed against the bore surface and allowed to remain in contact for approximately 1 h before removal using tweezers. The recovered replica was then placed on the microscope stage for surface texture examination using the optical microscope.

Microscopic evaluation was performed using a Nikon SMZ1270 stereomicroscope equipped with a Nikon Plan Apo 1× objective (WD 70 mm). A KoPa MC2000 digital camera system (Guangzhou Ostec Electronic Technology Co., Ltd., Guangzhou, China) was used for image acquisition at a nominal magnification of 8×. For each bore, one replica was evaluated from the predefined middle axial region on the front side. Six image locations were examined from each replica, consisting of two upper, two centre, and two lower image points.

The six images were treated as supporting observations of the same bore rather than six independent specimens. Therefore, a single bore-level evaluation was retained for the final surface-integrity assessment. This approach avoids artificially inflating the sample size while still allowing local surface features to be inspected across different portions of the replica.

The evaluation form included four principal inspection characteristics: cross-hatch line regularity, burr/kaeri condition, porosity or blowhole condition, and honing-line width. The cross-hatch angle was evaluated against the specified 30° ± 2° criterion. The inspection system considered a score of 3 or above acceptable for the defined line condition and burr/kaeri criteria, while the honing-width acceptance criterion was ≤30 µm.

Cross-hatch assessment was retained as both a numerical and inspection-based surface indicator. The cross-hatch angle can affect lubricant transport and ring–liner interaction; however, the functional behaviour of a honed surface is also influenced by groove continuity, spacing, depth, and local surface damage [6,9,16]. Microscopic inspection therefore complements numerical roughness measurements and helps distinguish general texture conditions from average roughness amplitude [21,22]. The complete replica-film preparation and microscopic evaluation sequence is shown in Figure 3.

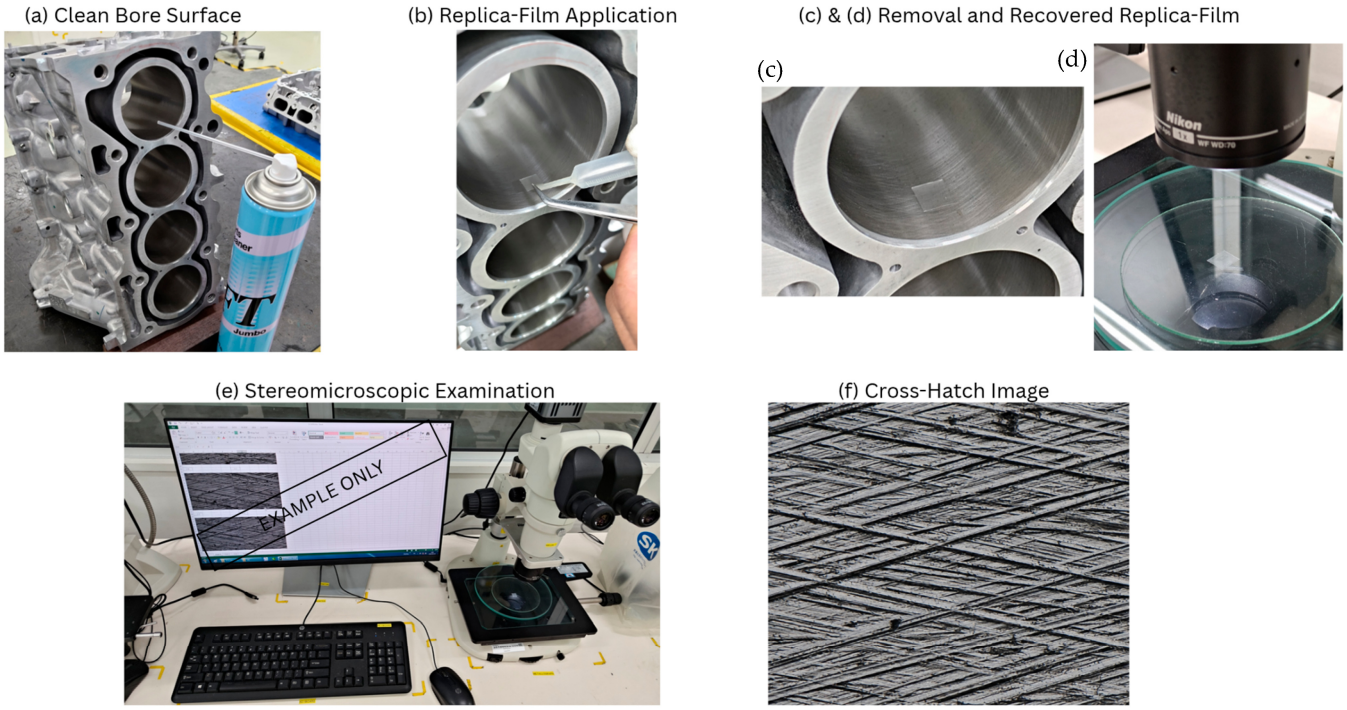

Figure 3. Replica film procedure used for cross-hatch surface characterisation: (**a**) cleaned bore surface; (**b**) application of replica film with ethyl acetate; (**c**) removal of the replica after the prescribed contact period; (**d**) recovered replica specimen; (**e**) stereomicroscopic examination at nominal 8× magnification; and (**f**) representative cross-hatch image used to assess angle, line condition, burr/kaeri, porosity/blowhole condition, and honing-line width.

For the comparative analysis, the recorded cross-hatch angle deviation and honing-line width were treated as numerical indicators, while the line condition, burr/kaeri, porosity/blowhole condition, and overall judgement were retained as surface-inspection indicators. The before-and-after difference in the numerical indicators was calculated using the same M2−M1 approach applied to the geometric and roughness measurements.

2.5. Dynamometer Test and Measurement Stages

All six engines were evaluated under the same controlled dynamometer operating condition. The principal comparison condition was established at 6000 rpm and 100% torque (full load). The same operating procedure and test arrangement were applied to both the ICE and HEV groups, and no abnormal test conditions were reported during the experimental runs. The 6000 rpm and 100% torque condition was selected as the controlled test point to provide consistent high-speed and full-load exposure for comparison between the two engine groups. This condition was not intended to reproduce the full range of operating conditions encountered during actual vehicle use.

All six engines followed the same dynamometer test sequence: engine warm-up, idle-timing measurement, full-load performance testing, mechanical-loss measurement, compression testing, oil-consumption testing, and blow-by measurement. During warm-up, the engine was held for 5 min after dynamometer torque became positive. It was then operated according to the model-specific RPM sequence specified in the monthly performance sheet, up to 6000 rpm. For idle-timing measurement, the engine was operated at 3000 rpm with an intake manifold pressure of −27 kPa until the oil and coolant temperatures reached 80 °C. The speed was then reduced to 1000 rpm for ignition-timing measurement. During full-load performance testing, the engine load was set to 100%, while engine speed and room temperature were checked for stability. At each prescribed RPM, two readings were

taken, with a 1 min waiting period before each recording. The repeat readings for each parameter were required to agree within 2%; otherwise, the measurement was repeated at that RPM.

The facility SOPs specify nominal durations of 1 h 55 min 30 s for full-load performance testing, 5 min 29 s for mechanical-loss measurement, and 15 min for compression testing. For mechanical-loss measurement, the engine was stabilised at 6000 rpm for 30 s before data were recorded over 6 s. For compression testing, the engine was motored at 350 rpm with the engine-load setting at 100%, and the reading was taken after 5 s. The oil-consumption assessment comprised a 2 h run and a separate 1 h run. These are nominal test durations; the total elapsed time for each engine could be longer because of warm-up, temperature conditioning, preparation, and repeated measurements.

Blow-by gas was measured after the engine oil temperature reached at least 80 °C. Measurements were taken at 6000 rpm and 4000 rpm, both at 100% torque, with three readings recorded at each speed using a Shinagawa wet gas meter (Tokyo Shinagawa Corporation, Tokyo, Japan; Model W-NK-5B). The facility SOP did not specify a fixed recording duration for each reading. For the principal comparison in this study, the final blow-by value was calculated as the arithmetic mean of the three readings obtained at 6000 rpm and expressed in L/min. The 4000 rpm readings were also recorded as part of the test procedure but were not used in the principal comparison. As blow-by reflects the response of the complete piston-ring sealing system, the measured values may also be influenced by engine speed, load, ring mobility, bore geometry, and other engine-related factors [3,10,23].

The oil consumption was measured at 6000 rpm and 100% engine load. The engine condition, oil temperature, and coolant temperature were monitored during the test. For the 2 h run, readings were recorded at the start and at 30 min intervals. The procedure was repeated in a separate 1 h run. Following the facility SOP, the final oil consumption value was calculated by subtracting the 2 h test result from the 1 h test result and dividing the difference by two. The results were expressed in g/h. Because oil consumption can arise from several sources, including the piston-ring pack, oil-film evaporation, valve-train components, crankcase ventilation, and oil drain-back, it was treated as an engine-level indicator rather than a direct measure of the cylinder-bore condition [11,24].

The use of controlled speed and load was intended to minimise operating condition variability during the ICE–HEV comparison. Therefore, the blow-by and oil-consumption results were interpreted together with the measured bore and surface conditions rather than as isolated measures of bore deformation. The dynamometer test configuration and monitored parameters are shown in Figure 4.

2.6. Experimental Calibration, Measurement Control, and Data Reliability

All dimensional and surface measurement instruments were operated using the facility's established calibration system. Equipment calibration was managed by the designated calibration team, with instruments maintained within their defined calibration validity periods. In addition, the calibration or measurement status of the equipment was checked before its use.

The Peacock No. 5 dial bore gauge was calibrated on 12 May 2026, and had a resolution of 0.001 mm. The calibration certificate recorded an overall result of "OK" for visual inspection, functionality, and performance. However, no separate uncertainty estimate for the complete measurement procedure was reported.

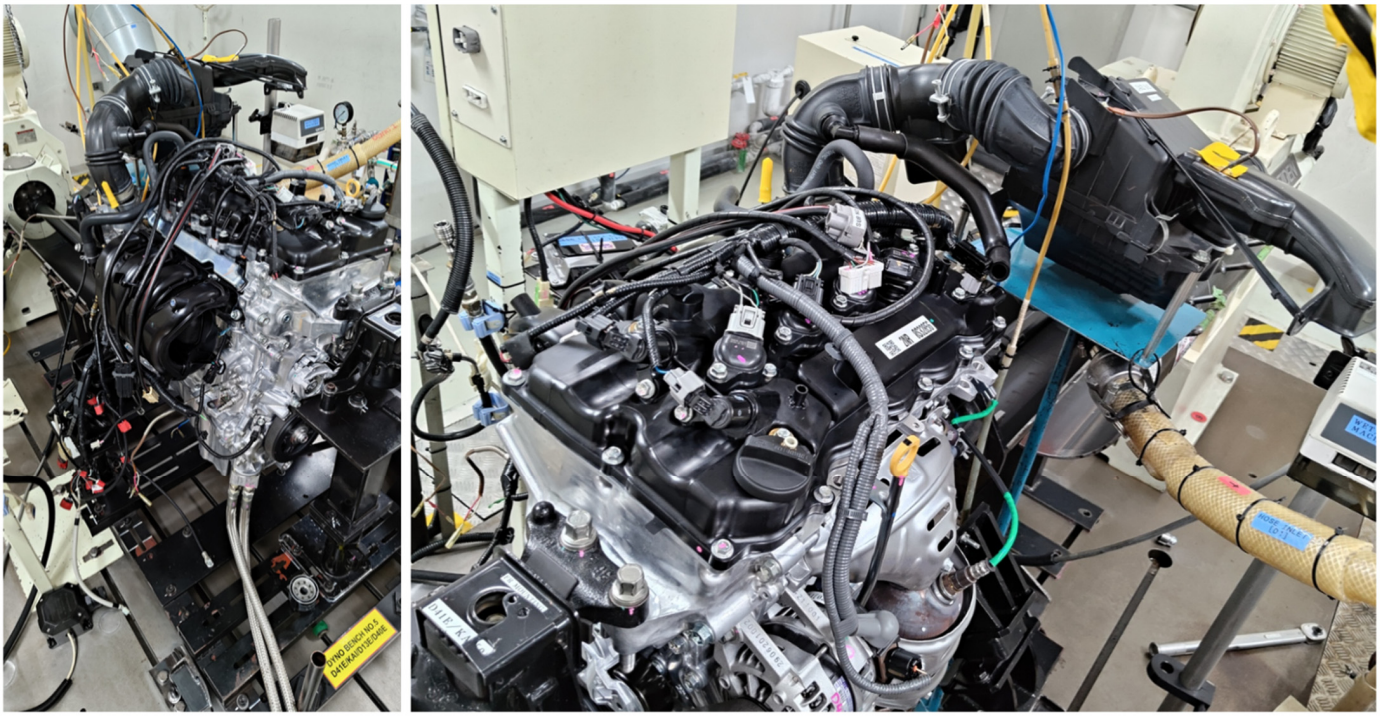

Figure 4. Engine dynamometer test setup used for controlled operation at 6000 rpm and 100% torque. The monitored parameters included engine speed and torque, oil and coolant temperatures, blow-by gas, oil consumption, cylinder compression, and facility-recorded fuel consumption.

The Mitutoyo Crysta-Apex S CMM had a maximum permissible length measurement error of $\pm(1.9 + 4\ L/1000)$ µm and a mean probing error of 1.2 µm. The expanded probing uncertainty was 0.25 µm ($k = 2$). For the Roncorder EC5100H roundness measurement system, the calibration results for the 15.00 µm master standard ranged from 14.96 to 15.03 µm, within the specified ±3% tolerance. The Mitutoyo Surftest SV-3100 was maintained under the facility's calibration system, and its calibration status was confirmed to be valid during both M1 and M2. However, model-specific numerical accuracy or uncertainty values were not available. Both measurement stages were conducted within the respective calibration validity periods, with intervals of less than one month.

Measurement consistency was controlled by using predefined measurement locations, fixed workpiece orientation, standardised reference directions, and consistent equipment settings. The same general measurement configuration was maintained between M1 and M2 to minimise the variation associated with repositioning and datum changes.

Manual bore-diameter measurements can be affected by the contact force, gauge centring, probe alignment, and handling technique. To maintain consistency between M1 and M2, the same operator performed both measurement stages using the same procedures. However, no independent operator repeatability studies have been conducted. Therefore, the extent of operator-related variation could not be determined.

For machine-based measurements, instrument calibration and fixed positioning were used as the principal controls. This approach recognises that calibration establishes confidence in instrument accuracy, while repeatability additionally depends on how the measurement procedure is executed. Previous metrology studies similarly emphasise the importance of measurement-system configuration, filtering, datum control, and measurement strategy when evaluating small dimensional changes [13,14,18–20].

No independent repeatability or reproducibility study was conducted for the complete measurement procedures. Consequently, the combined uncertainty of the M1–M2 measurements was not established. The calibration values reported in the individual certificates

describe specific instrument characteristics and should not be taken as the uncertainty of the complete measurement process. Therefore, small dimensional changes, particularly those close to the dial bore gauge resolution, were interpreted cautiously. Although the available calibration records and controlled measurement procedures support consistency between M1 and M2, they do not provide a formal estimate of the overall measurement uncertainty or establish compliance with all drawing tolerances.

2.7. Data Processing and Statistical Analysis

The dataset was organised hierarchically according to the engine, cylinder, axial location, measurement stage, and measurement parameter. The engine identifier was retained as the primary traceability key so that all cylinder-level geometry and surface measurements remained linked to the corresponding engine-level blow-by and oil-consumption results.

Measurement records were entered manually into Microsoft Excel 2016 (Microsoft Corporation, Redmond, WA, USA) for data organisation and subsequent analysis.

The primary comparison was the change between M1 and M2, which was calculated using Equation (1).

The resulting values were summarised using the mean, standard deviation, and range. Cylinder-level measurements were retained at the cylinder level for geometry, roughness, and cross-hatch assessment, whereas blow-by and oil consumption were treated exclusively as engine-level measurements.

The distinction between the measurement hierarchy and experimental replication was maintained throughout the analysis. The four cylinders within one engine were not treated as four independent engines. Instead, cylinder-level measurements were used to describe the within-engine bore and surface behaviour, while comparisons of engine-level sealing-related responses were based on the six independent engines.

Given the experimental sample size of three engines per group, ICE and HEV comparisons were interpreted primarily using descriptive statistics and the direction and magnitude of the measured changes. Statistical significance was not used as the sole basis for interpreting the engineering relevance. Instead, the comparison focused on the consistency of the observed response across multiple independent indicators, including geometry, roughness, crosshatch condition, blow-by, and oil consumption. Given the experimental design, individual engine variations may still contribute to the observed differences, and this limitation was considered when interpreting the ICE–HEV comparison. Where group-level standard deviations are reported in tables, they are calculated across the three independent engine-level means rather than treating individual cylinders or measurement locations as independent engines.

This integrated approach is consistent with the principle that bore geometry, surface texture, and sealing-related measurements provide different levels of evidence and should therefore be interpreted together rather than reduced to a single performance metric [1,2,5,10,11]. An exploratory association analysis was performed at the engine level by relating the mean changes in the selected bore geometry and surface roughness parameters to the corresponding blow-by and oil consumption values. Spearman 's correlation was used to assess monotonic associations. Because only six independent engines were available, the analysis was treated as exploratory, and the resulting associations were not interpreted as evidence of causation or population-level effects.

Spearman's rank correlation coefficient (ρ) ranges from -1 to $+1$. Its sign indicates the direction of the association, whereas its absolute value reflects the strength of the monotonic relationship. With only six independent engines, the coefficients were interpreted cautiously as exploratory findings and not as evidence of causation or effects that can be generalised to a wider engine population.

3. Results

Because the experimental design comprised three engines in each group, the results were primarily interpreted using descriptive comparisons between the pretest (M1) and post-test (M2) conditions. Cylinder-level measurements were retained for geometry and surface characterisation, whereas blow-by and oil consumption were evaluated at the engine level. Therefore, the four cylinders within an individual engine were not treated as independent engine replicates.

3.1. Changes in Cylinder-Bore Geometry

The geometric measurements showed that the dynamometer operation was accompanied by measurable changes in the bore size and form across the six engines. The magnitude and direction of the response varied between individual samples and geometric characteristics, indicating that the post-test bore condition was not represented by a single deformation mode.

As shown in Table 2, S1 exhibited a bore-diameter increase of 13.88 µm, compared with 2.33 µm for S2 and 2.38 µm for S3. This response raised the ICE group mean increase to 6.19 µm. When S1 was excluded for a sensitivity check, the mean change for the remaining two ICE engines was 2.36 µm, close to the HEV group mean of 2.71 µm. S1 was retained in the primary analysis; the additional calculation illustrates how strongly one engine influenced the ICE group mean. The difference in mean diameter change between the groups should therefore be interpreted in light of the observed engine-to-engine variability.

Table 2. Changes in the cylinder-bore geometric characteristics between M1 and M2. Group values are reported as mean ± SD across three independent engines.

Sample (Group)	Δ Diameter (µm)	Δ Ovality (µm)	Δ Taper (µm)	Δ Roundness (µm)	Δ Cylindricity (µm)	Δ Parallelism (µm)	Δ Straightness (µm)
S1 (ICE)	+13.88	+5.25	+2.00	+0.09	−1.35	+0.63	+0.57
S2 (ICE)	+2.33	+1.00	+2.50	+0.63	+2.18	+0.56	+1.22
S3 (ICE)	+2.38	+0.42	−1.50	+0.98	+1.08	+0.04	+1.25
S4 (HEV)	+2.88	+1.08	+2.25	+1.53	+3.05	+0.13	+0.82
S5 (HEV)	+2.58	+1.00	+1.50	+1.33	+0.98	+0.26	+1.01
S6 (HEV)	+2.67	+0.67	+2.25	+1.22	+1.98	+0.24	+1.00
ICE mean ± SD	6.19 ± 6.65	2.22 ± 2.64	1.00 ± 2.18	0.57 ± 0.45	0.63 ± 1.80	0.41 ± 0.32	1.01 ± 0.38
HEV mean ± SD	2.71 ± 0.15	0.92 ± 0.22	2.00 ± 0.43	1.36 ± 0.16	2.00 ± 1.04	0.21 ± 0.07	0.94 ± 0.11

A similar group-level difference was observed for the ovality. The ICE engines showed a mean increase of 2.22 µm, compared with 0.92 µm for the HEV engines. The taper response was smaller overall in this study. The ICE group showed a mean change of approximately +1.00 µm, whereas the HEV group showed a mean change of approximately +2.00 µm. S3 was the only engine showing a negative mean taper change of approximately −1.50 µm.

The form-related measurements produced a different pattern. The mean roundness increased by 0.57 µm for ICE and 1.36 µm for HEV. The mean cylindricity change was +0.63 µm for ICE and +2.00 µm for HEV. At the individual-engine level, the largest increase in cylindricity was observed for S4 at 3.05 µm, whereas S1 showed a reduction of 1.35 µm.

These results are consistent with the broader understanding that cylinder-bore distortion may contain several spatial components rather than a uniform change in bore size. Previous studies have shown that bore distortion can arise from combined structural, thermal, assembly, and operating loads, with different deformation patterns responding differently to the applied load conditions [25,26]. Thermal deformation studies of aluminium-alloy cylinder blocks have similarly identified roundness, cylindricity, and coaxiality as useful

indicators for describing the bore response under thermomechanical loading [27]. More recent work has also demonstrated that the cylinder-head bolt preload can produce measurable changes in the bore roundness and coaxiality before the engine is subjected to the operating loads [28].

Parallelism and straightness showed relatively small changes compared to the diameter and form characteristics. The mean parallelism change was 0.41 µm for ICE and 0.21 µm for HEV, while the corresponding straightness changes were 1.01 and 0.94 µm, respectively. Thus, although changes in bore-axis-related characteristics were detectable, the dominant differences between the groups were more evident in diameter, roundness, and cylindricity. The group-level changes across the principal geometric characteristics are compared in Figure 5.

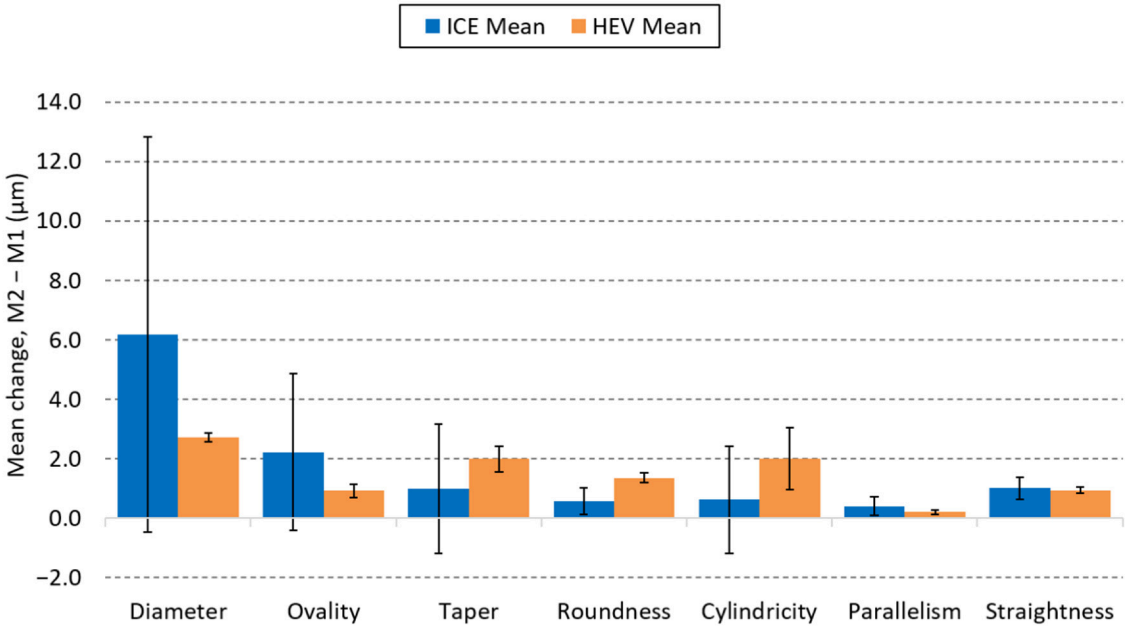

Figure 5. Group-level mean changes in cylinder-bore geometric characteristics between M1 and M2 for ICE and HEV engines. Diameter, ovality, and taper were converted from mm to µm for comparison on a common scale. Error bars represent the standard deviation of the three independent engine-level means in each group.

The variation among the geometric indicators demonstrates why the bore condition cannot be adequately represented by the diameter alone. For example, S1 showed the largest diameter and ovality changes but a relatively small roundness increase, whereas S4 showed a comparatively small diameter change but the largest cylindricity change. This difference highlights the importance of combining size- and form-based indicators when evaluating post-test bore conditions.

3.2. Surface Roughness Changes

The roughness measurements revealed a generally stronger reduction in the surface-profile amplitude parameters among the ICE engines than among the HEV engines. The most consistent changes were observed in Ra, Rz, Rk, Rpk, and Rvk, whereas the material-ratio parameters showed comparatively small changes.

For the ICE group, the mean Ra decreased from 0.393 to 0.345 µm, corresponding to a mean reduction of approximately 0.048 µm. The HEV group showed a much smaller decrease, from 0.373 to 0.366 µm, which is equivalent to approximately 0.008 µm. At the

sample level, all three ICE engines showed reductions in Ra, whereas S5 exhibited a very small increase of approximately 0.002 µm.

The change in Rz showed the same general trend. ICE engines exhibited a mean reduction of approximately 0.333 µm, whereas the HEV group showed a mean reduction of approximately 0.126 µm. The reduction in Rk was approximately 0.152 µm for ICE and 0.028 µm for HEV. Similarly, the mean Rpk reduction was approximately 0.060 µm for ICE, while the HEV group showed almost no change, at approximately −0.001 µm.

Rvk decreased by approximately 0.085 µm for ICE and 0.010 µm for HEV. These changes indicate that the ICE surfaces experienced a more noticeable modification in peak, core, and valley-related amplitude characteristics after the test. This result is consistent with the functional nature of honed surfaces, where running-in can modify surface asperities and the associated profile parameters even when the overall honing pattern remains recognisable [23,29–31].

The material-ratio parameters exhibited smaller changes. Mr1 increased slightly from approximately 8.33% to 8.54% for ICE and from 8.37% to 8.44% for HEV, while Mr2 showed small decreases of approximately 0.05 percentage points for ICE and 0.15 percentage points for HEV. These relatively small changes suggest that the principal surface response in the present experiment was more apparent in the amplitude-related parameters than in the overall material-ratio distribution. The corresponding M1–M2 roughness comparison is presented in Figure 6 and summarised numerically in Table 3.

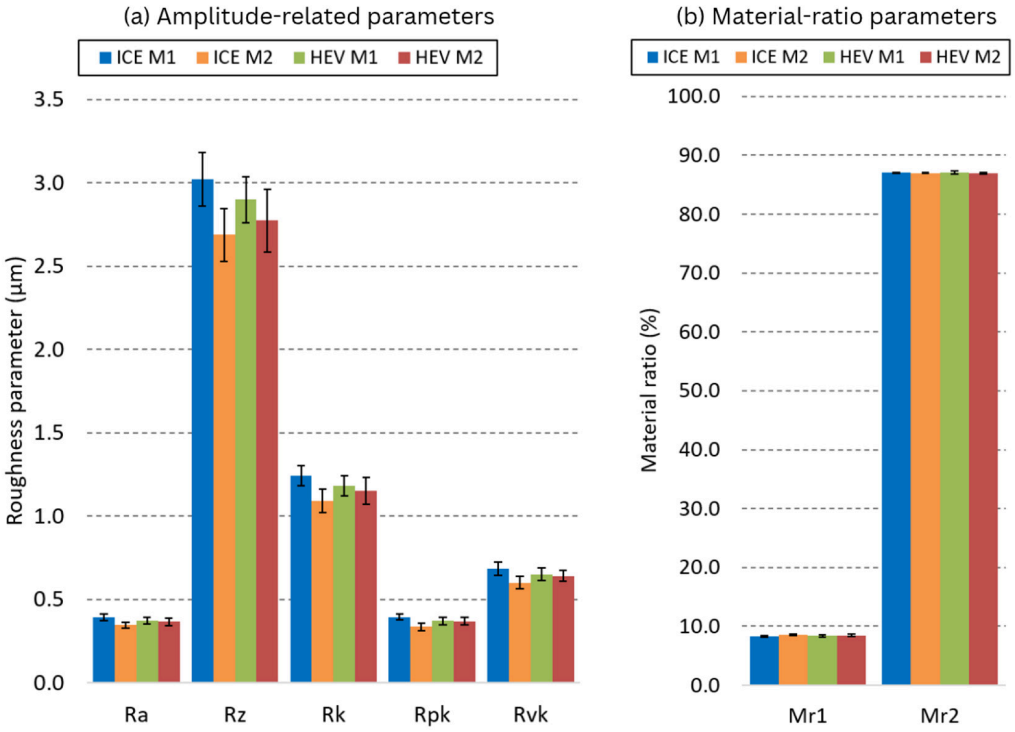

Figure 6. Group-level surface roughness results before (M1) and after (M2) dynamometer operation: (**a**) amplitude-related parameters Ra, Rz, Rk, Rpk, and Rvk; and (**b**) material-ratio parameters Mr1 and Mr2. Error bars represent the standard deviation across three independent engine-level means in each group.

Table 3. Group-level cylinder-bore surface roughness results. Values are mean ± SD across three engine-level means for each engine group.

Parameter	ICE M1	ICE M2	Δ ICE	HEV M1	HEV M2	Δ HEV
Ra (µm)	0.393 ± 0.019	0.345 ± 0.019	−0.048 ± 0.013	0.373 ± 0.020	0.366 ± 0.023	−0.008 ± 0.010
Rz (µm)	3.020 ± 0.161	2.687 ± 0.157	−0.333 ± 0.080	2.899 ± 0.138	2.773 ± 0.187	−0.126 ± 0.064
Rk (µm)	1.242 ± 0.060	1.090 ± 0.071	−0.152 ± 0.039	1.180 ± 0.061	1.152 ± 0.079	−0.028 ± 0.022
Rpk (µm)	0.394 ± 0.018	0.335 ± 0.022	−0.060 ± 0.016	0.370 ± 0.022	0.368 ± 0.023	−0.001 ± 0.009
Rvk (µm)	0.684 ± 0.038	0.600 ± 0.038	−0.085 ± 0.026	0.651 ± 0.037	0.641 ± 0.031	−0.010 ± 0.016
Mr1 (%)	8.330 ± 0.142	8.544 ± 0.157	0.215 ± 0.227	8.368 ± 0.159	8.445 ± 0.210	0.077 ± 0.280
Mr2 (%)	87.006 ± 0.091	86.957 ± 0.037	−0.049 ± 0.080	87.056 ± 0.253	86.906 ± 0.148	−0.150 ± 0.285

The difference in response between the two groups is particularly evident when Ra is considered together with Rz, Rk, Rpk, and Rvk. Rather than showing an isolated change in average roughness, the ICE group exhibited a broader reduction across several amplitude-related indicators. This supports the use of a multi-parameter surface description because plateau-honed surfaces contain distinct peaks, cores, and valleys that are not fully represented by Ra alone [5,14,23].

3.3. Cross-Hatch Surface Condition

The cross-hatch inspection showed that the bore surfaces remained within the specified inspection requirements after dynamometer operation. All evaluated cylinders retained an overall evaluation score of 3, corresponding to the acceptable condition defined by the inspection procedure. The cross-hatch line condition and burr/kaeri scores likewise remained at 3 throughout the dataset. The sample-level before-and-after cross-hatch measurements are presented in Figure 7, while the numerical and inspection outcomes are summarised in Table 4.

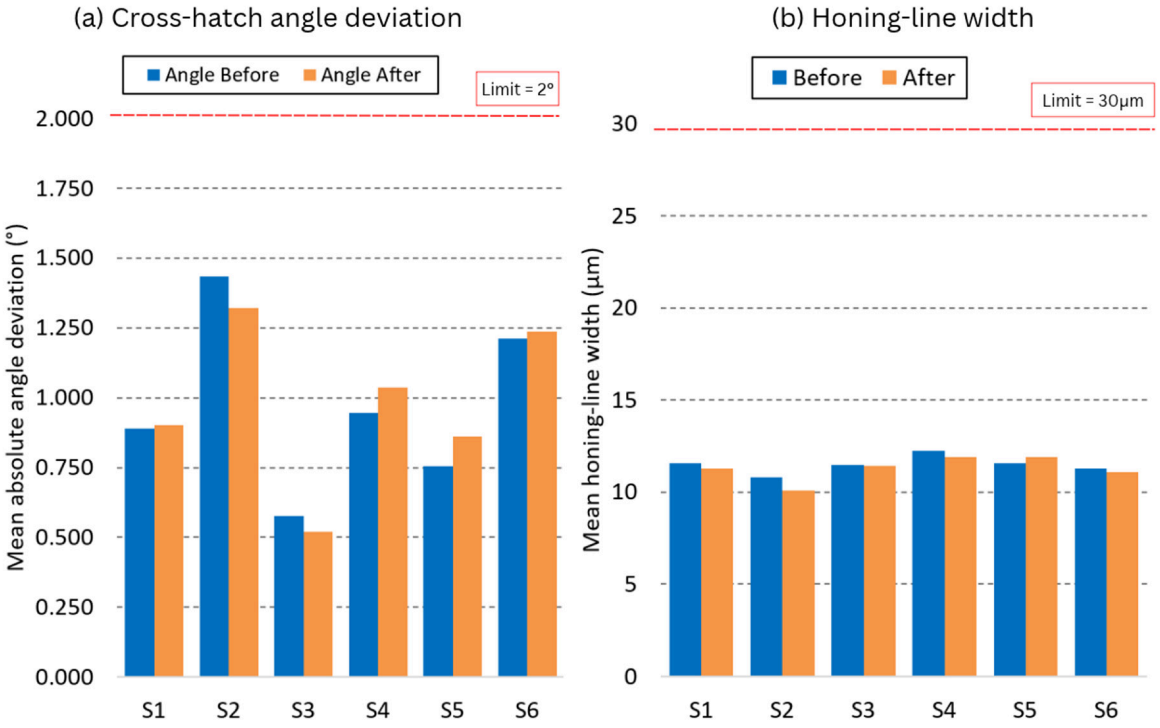

Figure 7. Sample-level before-and-after cross-hatch measurements: (**a**) mean absolute cross-hatch angle deviation for each engine, with the 2° acceptance limit shown by the dashed line; and (**b**) mean honing line width, with the 30 µm acceptance limit shown by the dashed line.

Table 4. Cross-hatch and honing-surface results for the ICE and HEV groups. Continuous values are mean ± SD across three engine levels; porosity values are counts.

Parameter	ICE Before	ICE After	HEV Before	HEV After
Mean absolute angle deviation (°)	0.966 ± 0.434	0.915 ± 0.401	0.971 ± 0.230	1.044 ± 0.189
Mean angle deviation (°)	−0.079 ± 0.141	−0.012 ± 0.130	0.128 ± 0.168	0.192 ± 0.253
Mean honing width (µm)	11.29 ± 0.43	10.94 ± 0.73	11.70 ± 0.49	11.63 ± 0.46
Total porosity observations	0	0	1	1
Overall score	3	3	3	3
Overall judgement	OK	OK	OK	OK

For the ICE group, the mean absolute cross-hatch angle deviation decreased slightly from 0.966° before testing to 0.915° after testing. In contrast, the HEV group showed an increase from 0.971° to 1.044°. Despite these changes, all measurements remained below the specified 2° acceptance range.

The honing line width exhibited a smaller response. The ICE group decreased from a mean of 11.29 µm to 10.94 µm, whereas the HEV group changed from 11.70 µm to 11.63 µm. All measured honing line widths were below the specified 30 µm limit.

Two porosity observations were recorded in the HEV dataset: one after testing S5 and one before testing S6. No porosity was recorded for S5 before testing or for S6 after testing, and no porosity was observed in the ICE group. Because these were isolated observations rather than repeated defects across groups, they were reported descriptively and were not interpreted as evidence of a systematic group-level trend.

Therefore, the numerical changes in the cross-hatch angle and honing width did not occur with a corresponding transition in the overall inspection judgement. This distinction is relevant because the microscopic surface condition and functional surface texture cannot necessarily be represented completely by a binary acceptable/not-acceptable assessment. Experimental studies have shown that surface texture characteristics can influence cylinder liner/piston ring performance under real engine conditions, whereas localised surface damage may affect friction and wear without necessarily removing the overall honing pattern [29,30].

The cross-hatch results are therefore best interpreted as evidence that no gross deterioration of the evaluated honing pattern was detected, rather than as evidence that the bore surface remained unchanged. The simultaneous roughness results provide evidence that the numerical surface characteristics changed even though the conventional cross-hatch acceptance status remained unchanged.

3.4. Blow-By Gas and Oil Consumption

Engine-level measurements showed that all six engines remained within the applicable acceptance limits for both blow-by and oil consumption. The blow-by values ranged from 17.72 to 20.39 L/min, compared with the specified limit of 23.6 L/min. The oil consumption values ranged from 7.84 to 11.91 g/h, compared with the limit of 35.6 g/h.

Within the ICE group, the mean blow-by value was 19.62 L/min, whereas the corresponding HEV value was 18.20 L/min. The difference between the two groups was approximately 1.42 L/min. For oil consumption, the ICE mean was 10.76 g/h, compared with 8.75 g/h for the HEV, corresponding to a group difference of approximately 2.01 g/h.

At the individual-engine level, S3 had the highest blow-by and oil consumption values, at 20.39 L/min and 11.91 g/h, respectively. The lowest values were recorded for S5, with 17.72 L/min blow-by and 7.84 g/h oil consumption.

These engine-level responses should be interpreted as overall sealing and oil control indicators rather than direct measurements of the cylinder bore condition. Blow-by is

affected by the complete ring-sealing system, including the ring geometry, mobility, ring gap, combustion pressure, and bore condition [10,32]. Oil consumption involves multiple potential pathways and is influenced by the measurement procedure, oil film behaviour, evaporation, drainback, and other engine components [11,24]. The engine-level blow-by and oil consumption results for all six engines are shown in Figure 8.

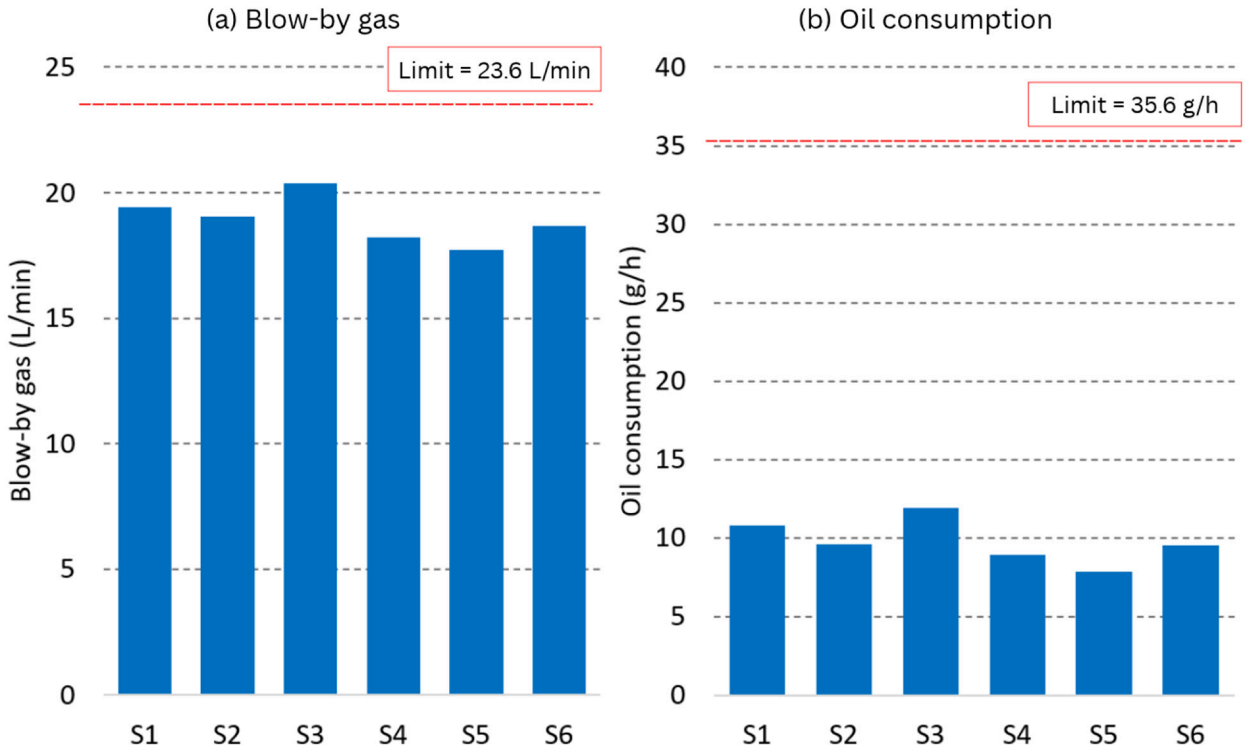

Figure 8. Engine-level sealing-related indicators under controlled dynamometer conditions: (**a**) blow-by gas and (**b**) oil consumption for samples S1–S6. The dashed lines indicate the applicable acceptance limits of 23.6 L/min and 35.6 g/h, respectively.

The engine-level sealing-related measurements are summarised in Table 5.

Table 5. Engine-level blow-by and oil consumption results. Group values are the mean ± SD for n = 3 engines.

Sample	Blow-by (L/min)	Blow-by Limit (L/min)	Oil Consumption (g/h)	Oil-Consumption Limit (g/h)	Judgement
S1 (ICE)	19.43	23.6	10.78	35.6	PASS
S2 (ICE)	19.04	23.6	9.60	35.6	PASS
S3 (ICE)	20.39	23.6	11.91	35.6	PASS
S4 (HEV)	18.21	23.6	8.90	35.6	PASS
S5 (HEV)	17.72	23.6	7.84	35.6	PASS
S6 (HEV)	18.67	23.6	9.51	35.6	PASS
ICE mean ± SD	19.62 ± 0.69	—	10.76 ± 1.16	—	—
HEV mean ± SD	18.20 ± 0.48	—	8.75 ± 0.85	—	—

The results indicate that the difference between the groups was more apparent in the engine-level sealing-related measurements than in the cross-hatch acceptance judgement. However, because only three independent engines were available per group, the observed ICE–HEV differences are treated as descriptive experimental differences rather than statistically generalised group effects.

3.5. Integrated Comparison of Bore Geometry, Surface Integrity, and Sealing-Related Indicators

The combined results revealed that the post-test bore condition changed at multiple measurement levels, although the magnitude and direction of the response differed between the ICE and HEV groups.

Therefore, the combined observations show that the measurement domains did not respond in an identical manner. Bore geometry provided direct evidence of dimensional and form changes, roughness measurements quantified surface-profile modification, cross-hatch inspection assessed the retention of the honing pattern, and blow-by and oil consumption provided broader engine-level responses.

The absence of a one-to-one correspondence among these domains is itself an important result: a larger change in one geometric or roughness parameter did not necessarily coincide with a loss of cross-hatch acceptance or with the highest engine-level sealing response. A similar multi-level approach has been advocated in studies examining the relationship between liner texture, ring interaction, and engine performance, where the surface condition cannot be interpreted independently of the operating system [29,30]. The integrated comparison of these measurement domains is shown in Figure 9.

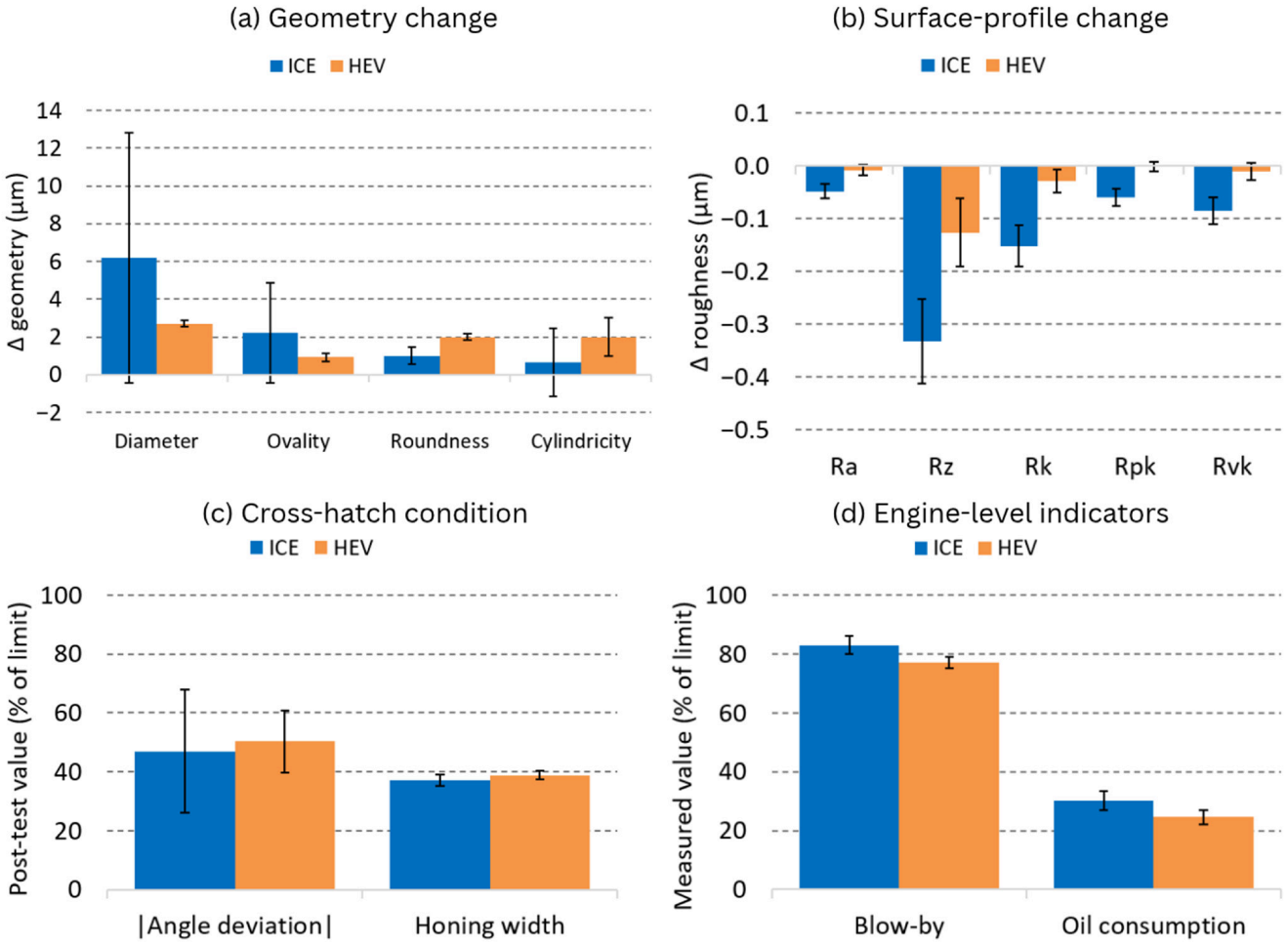

Figure 9. Integrated group-level comparison across the principal measurement domains: (**a**) selected changes in bore geometry, (**b**) changes in amplitude-related roughness parameters, (**c**) post-test cross-hatch angle deviation and honing-line width expressed as percentages of their respective acceptance limits, and (**d**) blow-by and oil consumption expressed as percentages of their respective acceptance limits. Error bars represent the standard deviations of three independent engines per group.

The results also show why an individual parameter should not be used as a standalone indicator of bore condition. For example, S1 produced the largest diameter change but did not exhibit the largest increase in roundness or cylindricity. Conversely, S4 exhibited a relatively small diameter change but the largest cylindricity increase. Similarly, the HEV group retained acceptable cross-hatch scores despite showing measurable geometric changes and smaller but detectable changes in several roughness parameters.

Therefore, the experimental findings support a multiparameter interpretation in which geometry, surface integrity, and engine-level sealing indicators are considered together. The association between these variables is further examined in the Section 4.

4. Discussion

4.1. Bore Geometric Response After Dynamometer Operation

The experimental results demonstrate that the cylinder-bore response after dynamometer operation was multidimensional rather than being represented by a uniform change in bore size. The ICE group showed a larger mean increase in diameter and ovality, whereas the HEV group exhibited larger mean changes in roundness and cylindricity. This difference is important because it indicates that the post-test response cannot be adequately described by a single-dimensional indicator.

The individual-engine results also highlight the influence of engine-to-engine variability on group-level comparisons. Despite the common dynamometer test procedure and the use of the same operator for both M1 and M2 measurements, the magnitude of diameter change varied considerably among the engines. As discussed in Section 3.1, S1 showed a substantially larger increase than the other two ICE engines. However, no abnormality or rework was identified in the available production records for S1; therefore, the cause of its larger response could not be established from the present data. The engines also originated from different production dates and batches. Given the small sample size, batch-related effects cannot be separated from engine-specific variability. The observed ICE–HEV differences should therefore be interpreted as descriptive findings for the six tested engines, rather than as general differences between the two engine designs.

Previous numerical studies have used finite element analysis (FEA) and thermo-mechanical modelling to examine cylinder bore deformation under assembly and operating thermal conditions. Bhosale et al. [26] used FEA to investigate bore distortion caused by cylinder head bolt clamping. Bao et al. [27] developed a thermo-mechanical coupling model to assess deformation under different material and thermal conditions, while Li et al. [28] examined the effect of bolt preload using a coupled model of the cylinder head, gasket, cylinder block, and bolts. Wang et al. [33] investigated the axial and radial deformation of a cylinder liner under rated firing conditions using a fully coupled thermo-mechanical model. The modelling approaches and principal findings of these studies are summarised in Table 6.

Collectively, these studies demonstrate that cylinder-bore deformation depends on the applied loading conditions and the structural and thermal characteristics of the engine assembly. The findings support the use of multiple geometric indicators when interpreting bore-condition changes, as a single-dimensional parameter may not capture the full deformation pattern.

The differences between diameter, roundness, and cylindricity changes are particularly informative. S1 exhibited the largest diameter and ovality changes but only a small roundness change, whereas S4 showed a much larger increase in cylindricity despite its relatively small diameter change. This behaviour reinforces the distinction between size, cross-sectional form, and three-dimensional cylindrical form. A change in diameter does

not necessarily imply an equivalent change in roundness, and a small diameter shift can coexist with a measurable change in axial or three-dimensional form [12,13,25].

Table 6. Summary of numerical modelling approaches, simulation conditions, and reported cylinder-bore deformation findings in previous studies.

Study	Modelling Approach and Conditions	Main Reported Findings
Bhosale et al. [26]	MSC NASTRAN FEA; three-cylinder inline diesel engine; cylinder-head bolt clamping loads with variations in bolt pretension.	Increasing bolt pretension affected the bore deformation harmonics, with the fourth-order component being more sensitive than the second-order component. The predictions showed fair agreement with the previously reported experimental results.
Bao et al. [27]	Thermo-mechanical coupling model comparing cast iron and aluminium-alloy cylinder blocks. Model reliability was assessed using measured temperature field data.	Under thermo-assembly conditions, the average roundness, cylindricity, coaxiality, and light-leakage rate of the aluminium-alloy cylinder bore were higher by 36.71%, 12.69%, 14.77%, and 18.85%, respectively, compared to the cast-iron cylinder bore.
Li et al. [28]	Coupled cylinder head, gasket, cylinder block, and bolt model focusing on bolt preload	Compared with the cast-iron block, the aluminium-alloy block showed 54.41% higher average roundness and 27.08% higher coaxiality. After optimisation of the cylinder-head bolted-coupling parameters, the average roundness and coaxiality decreased by 38.79% and 36.07%, respectively, compared with the original block configuration.
Wang et al. [33]	Fully coupled thermo-mechanical model of a wet cylinder liner in a non-road diesel engine under rated firing conditions	Segmented pre-compensation design reduced the maximum axial straightness deviation by approximately 18%, while the roundness remained nearly unchanged.

Notes: The reported numerical results correspond to the respective engine configurations, material systems, loading conditions, and comparison baselines used in each study. These should not be interpreted as direct quantitative benchmarks for the experimental M1–M2 changes reported in the present study.

The present results are also consistent with studies that show that bore distortion is spatially dependent. Yang et al. demonstrated that cylinder-liner distortion contains multiple geometric components associated with the deformation spectrum of the liner [25]. Similarly, previous dimensional inspections of cylinder liners have shown that diameter, roundness, centre location, and axis-related characteristics can vary along the liner rather than changing uniformly over its length [4,13]. This supports the multi-region measurement strategy used in the present study.

From an engineering perspective, the observed changes should therefore be interpreted as changes in bore condition, rather than as a single scalar measure of "deformation severity." The diameter and ovality provide information about size and directional distortion, roundness describes the local circumferential form, and cylindricity provides a broader description of the three-dimensional bore shape. Their combined interpretation is more informative than that of any single parameter [4,12,13].

An additional consideration is that the post-test measurements represent the combined effect of the engine's pre-existing condition and subsequent operating exposure. The head-bolt preload and assembly related distortion may have already influenced the bore before the dynamometer test. Previous experimental and numerical studies have shown that the

bolt preload can measurably alter the cylinder-bore geometry in aluminium-alloy engine blocks [28]. Therefore, the M1–M2 difference should be interpreted as the net change between the defined pre- and post-test states, rather than as a measurement of thermal loading alone.

4.2. Surface Roughness Modification and Running-In Behaviour

The surface measurements indicated that dynamometer operation was accompanied by a more noticeable reduction in amplitude-related roughness parameters for the ICE group than for the HEV group. In particular, Ra, Rz, Rk, Rpk, and Rvk decreased more clearly for ICE. This pattern suggests that the surface response extended beyond a simple change in average roughness.

One possible interpretation is that the measured changes are associated with early surface modification or running-in of the honed bore. Plateau-honed surfaces contain relatively prominent peaks, a load-bearing core, and deeper valleys. During sliding exposure, some asperity peaks may be preferentially modified, whereas the underlying valley structure remains comparatively stable [5,31]. Experimental studies of cylinder-liner/piston-ring systems have also shown that surface texture can influence tribological behaviour during the running-in process [34].

The reduction in Rpk is particularly relevant in this context because Rpk describes the reduced peak height above the core region. Therefore, a reduction in Rpk can be consistent with the modification of the higher asperity population during running-in, although the present experiment did not directly isolate running-in from other possible surface effects. Similar changes in the plateau-surface characteristics during running-in have been investigated using automated surface-evaluation approaches [31,35].

However, the present measurements do not allow beneficial running-in or plateauing to be distinguished definitively from undesirable wear because direct material loss or wear-volume measurements were not performed. Therefore, the reduction in roughness parameters was interpreted as evidence of surface modification that is consistent with possible running-in, rather than as direct evidence of beneficial wear. The acceptable cross-hatch condition further indicates that no gross deterioration of the honing pattern was detected; however, it does not exclude localised material removal or wear. Recent experimental work on honed cylinder-liner failure has shown that undesirable surface wear can involve abrasive–corrosive mechanisms under inadequate lubrication and contaminant exposure [36].

The reduction in Rvk was smaller but still measurable for the ICE group. Because Rvk characterises the reduced valley region, its response is relevant to the lubricant-retention characteristics of a honed surface. However, a reduction in Rvk should not automatically be interpreted as deterioration of lubrication. Valley functionality depends on the complete texture, including groove geometry, spacing, continuity, and oil transport pathways [6,16].

This observation is consistent with the literature on surface textures. Pawlus et al. emphasised that plateau-honed cylinder liners should be characterised using multiple parameters because different parts of the profile have different functional roles [5]. Walid and Eifler highlighted the importance of selecting surface characterisation methods according to the functional question rather than relying on a single conventional roughness parameter [14]. In this study, the simultaneous reduction in Ra, Rz, Rk, Rpk, and Rvk provided a more informative description of the post-test surface modification than Ra alone.

4.3. Cross-Hatch Acceptance Versus Functional Surface Change

One of the most important findings of this study is that the crosshatch surface remained within the specified acceptance criteria despite measurable changes in bore geometry and roughness.

The overall cross-hatch evaluation remained at an acceptable score of 3 for both pre-test and post-test conditions. The honing-line widths also remained well below the specified 30 µm limit. The mean absolute angle deviation remained below the specified 2° tolerance for both engine groups. Thus, the conventional inspection system detected no gross deterioration in the cross-hatch condition.

However, the surface roughness results showed measurable post-test changes. This apparent difference between the inspection judgement and quantitative roughness response is not contradictory. The two methods characterise different aspects of the surface. The cross-hatch evaluation is primarily concerned with the compliance of the honing pattern and the presence of visually or geometrically significant defects, whereas the roughness parameters describe the statistical characteristics of the surface profile at the measurement trace.

The same distinction has been discussed in previous surface-texture studies. The cross-hatch angle alone does not define complete surface functionality because groove spacing, depth, continuity, and local defects also influence lubricant transport and ring interaction [6,9,16]. Similarly, localised grinding or honing irregularities can affect friction and wear, even where the overall surface remains recognisably honed [30].

The present results suggest that conventional cross-hatch acceptance criteria are useful for identifying gross surface defects but may be less sensitive to subtle quantitative changes during engine operation. A cylinder can remain within the acceptance criteria while showing measurable changes in roughness and geometry.

However, an acceptable cross-hatch score should not be interpreted as evidence that no wear occurred, as the acceptance criteria primarily indicate that no gross deterioration of the evaluated honing pattern was detected. For research-level condition monitoring, the existing cross-hatch criteria could therefore be supplemented with quantitative parameters such as Ra, Rz, Rk, Rpk, Rvk, cross-hatch angle deviation, and honing-line width. This combined approach retains the existing acceptance criteria while providing greater sensitivity to gradual surface changes.

The microscopic replica method also provided complementary evidence. Rather than treating the six microscopic image points as independent experimental observations, they were used to characterise different portions of the same cylinder-bore surface and produce one bore-level evaluation. This preserves the spatial information available from the surface while avoiding pseudoreplication.

This result is particularly relevant when interpreting sealing-related behaviour. The preservation of an acceptable cross-hatch pattern does not automatically imply that all ring–liner conditions remained unchanged. Ring motion, local surface texture, bore form, oil-film behaviour, and operating conditions can change while the general honing pattern remains intact [2,3,10].

4.4. Relationship Between Bore Geometry and Surface Integrity

The combined geometry and roughness results indicate that dimensional and surface responses were related but not identical. The ICE group exhibited a relatively large change in mean diameter and a stronger reduction in roughness amplitude parameters, whereas the HEV group exhibited smaller diameter changes but larger average roundness and cylindricity changes.

This lack of one-to-one correspondence is physically reasonable. Bore geometry describes the macroscopic location and shape of the bore surface, while roughness characterises much smaller-scale topographical features. A change in bore diameter does not necessarily imply a proportional change in surface texture, and vice versa. Therefore, the two measurement domains represent different spatial scales of the same functional surface.

Previous studies have treated these scales separately when modelling the ring–liner system. Three-dimensional contact modelling has shown that bore geometry influences ring conformity and separation behaviour [3], whereas surface-texture studies have shown that roughness, honing grooves, and local surface structure influence lubrication and friction [5,6,16]. Their effects can therefore coexist without necessarily changing in the same direction.

The observed changes in S1 provide a useful example. The sample exhibited the largest diameter change and the largest ovality increase, yet its roundness change was comparatively small. This indicates that the dimensional response was not a uniform enlargement of the bore. Conversely, S4 exhibited the largest roundness and cylindricity changes, while its diameter change remained close to the range of the other samples. Such behaviour reinforces the importance of separating size-based and form-based indicators.

This interpretation is consistent with previous studies showing that sealing and ring–bore interaction depend on geometric profile characteristics rather than on a single bore diameter value [2,3]. Accordingly, the present results support a multi-scale interpretation in which geometric forms and surface textures should be considered complementary indicators.

4.5. Association with Blow-By Gas

The blow-by results provide an engine-level indication of the overall sealing condition after the dynamometer operation. The HEV group showed a lower mean blow-by value than the ICE group, whereas all engines remained below the specified acceptance limit.

However, the observed group difference should not be interpreted as evidence that the HEV bore geometry directly produced lower blow-by. Blow-by is a system-level response involving combustion pressure, ring dynamics, ring gap, ring mobility, bore geometry, and gas-flow characteristics of the complete ring pack [3,10,23].

Previous studies have demonstrated that piston ring mobility can affect gas passage through the ring pack, and that ring motion and pressure distribution change with engine operating conditions [10,23,32]. Cheng et al. demonstrated through three-dimensional modelling that local bore geometry influences the interaction between the ring and cylinder wall [3]. These studies provide a physical basis for considering bore geometry as a contributor to sealing behaviour, but not as the sole determinant.

The present dataset illustrates this point. S3 exhibited the highest blow-by value among the six engines, while several of the geometric changes observed in that engine were not the largest values in the dataset. Conversely, S1 displayed the largest mean diameter change but did not produce the highest blow-by. This absence of a simple monotonic relationship indicates that engine-level sealing behaviour is influenced by multiple interacting variables.

Therefore, the appropriate interpretation is one of association rather than direct causation. The measured bore and surface changes provide condition evidence that can be examined alongside blow-by, while the blow-by result provides a broader indication of the sealing response. This evidence hierarchy is more defensible than attributing the engine-level response to a single geometric parameter. Because blow-by was measured at the engine level, the present data do not allow the response of an individual cylinder to be directly linked to the measured blow-by value.

An exploratory engine-level association analysis showed stronger monotonic relationships between several roughness changes and blow-by than between the main geometric parameters. The changes in Ra, Rz, and Rk each showed a Spearman correlation of −0.943 with blow-by, whereas Rpk and Rvk showed correlations of −0.886. Roundness showed a weaker negative association ($\rho = -0.771$), whereas diameter and cylindricity showed weak negative associations ($\rho = -0.143$ and -0.257, respectively). These relationships are exploratory only, as the analysis was based on six independent engines and may also reflect the separation between ICE and HEV groups.

4.6. Association with Oil Consumption

The HEV group also showed a lower mean oil consumption value than the ICE group. This difference occurred while both groups maintained an acceptable cross-hatch condition and while measurable differences in bore geometry and surface roughness were observed.

Oil consumption is inherently more complex than blow-by because it can involve several pathways, including oil transport through the ring pack, oil-film evaporation, valve guides and seals, crankcase ventilation, drain-back, and other engine components [11,24]. Consequently, a reduction in oil consumption cannot be interpreted as direct evidence of reduced bore deformation or improved cross-hatch condition. In particular, oil transport within the ring pack is closely coupled with gas flow and blow-by behaviour [37].

The relationship between surface texture and oil control is nevertheless relevant. Honed-surface characteristics influence lubricant retention and ring–liner interaction, while oil consumption reflects the interacting ring-pack and lubricant-transport mechanisms [6,11,24]. These mechanisms provide a physical basis for considering surface condition together with oil-consumption response, without treating either measurement as a direct proxy for the other.

Recent studies have examined the cylinder-liner/piston-ring surface topography under different temperature and load conditions [38] and tribofilm formation and distribution at the ring–liner interface under realistic engine operating conditions [39]. Reviews have also discussed advances in surface texturing and coating technologies for improving the tribological performance and durability of this system [40]. These studies provide a broader tribological context for interpreting roughness and cross-hatch observations in the present work. However, they did not establish that the measured surface changes caused differences in oil consumption among the six engines.

Therefore, the oil consumption results in the present study are best treated as supporting evidence of the overall engine oil control behaviour. The measured values can be discussed together with the roughness and geometric results; however, they should not be used independently to identify a specific deformation mechanism. Similarly, the engine-level oil consumption result cannot be assigned to a specific cylinder or local bore feature.

The exploratory engine-level analysis showed a similar pattern for oil consumption. Changes in Ra, Rz, and Rk showed Spearman correlations of −0.943 with oil consumption, while Rpk and Rvk showed correlations of −0.886. Roundness showed a weaker negative association ($\rho = -0.771$), whereas diameter and cylindricity showed weak associations ($\rho = -0.143$ and -0.257, respectively). These results suggest that the roughness-related changes may warrant further investigation in relation to engine-level oil-control behaviour; however, the small number of engines does not allow these associations to be interpreted as independent or causal relationships.

4.7. ICE and HEV Comparative Behaviour

Therefore, the comparison should be interpreted in the context of the experimental design and controlled test conditions. The engines were evaluated under the same controlled continuous dynamometer condition, which reduces one source of experimental variability and supports a direct descriptive comparison. However, this condition does not reproduce the HEV-specific operating characteristics, such as start–stop events and varying duty cycles. Therefore, the present comparison reflects the response of the two engine groups under the same controlled operating exposure rather than their full real-world operating behaviour. Nevertheless, three engines per group remained a small experimental population, and the present study was not designed to establish population-level statistical differences.

The different geometric responses may also reflect differences in engine structural configuration, assembly condition, thermal history, and operational design characteristics. Previous research has shown that cylinder-bore deformation depends on the interaction between the thermal and mechanical fields and the structural constraints imposed on the cylinder block [25–28]. In the present study, the main bore geometry, dimensions, and material standards were closely matched between the ICE and HEV engines, whereas differences remained in the block design and the location used to monitor the coolant inlet temperature.

The larger diameter and ovality changes observed in the ICE group indicate a greater dimensional and directional response, whereas the larger roundness and cylindricity changes in the HEV group indicate a greater change in local cross-sectional and three-dimensional bore form. These contrasting deformation responses may be influenced by differences in structural constraints, head-bolt loading, and local thermal distribution. However, these factors were not independently measured in the present study. Therefore, the observed differences should be interpreted in consideration of these engine-specific characteristics rather than being attributed solely to the ICE–HEV category.

Mechanistically, non-uniform thermal expansion or local structural restraint may produce measurable changes in roundness or cylindricity without producing a similarly large change in mean diameter. Conversely, a more pronounced directional response may appear as increased diameter and ovality. These interpretations remain qualitative because the present experimental program was not designed to isolate the individual effects of block stiffness, bolt loading, and thermal distribution.

The surface results add another layer to the comparison. A stronger reduction in the amplitude-related roughness parameters for ICE occurred without a corresponding deterioration in the cross-hatch acceptance. This suggests that the two groups may experience different degrees of surface evolution while maintaining the same broad honing pattern compliance.

The present findings therefore support a more cautious conclusion: the ICE and HEV groups demonstrated different post-test combinations of geometric deformation, surface modification, and sealing-related responses under the investigated dynamometer condition. The data do not justify reducing this behaviour to a simple statement that one group universally produces better or worse bore performance.

4.8. Practical Implications and Current Applicability

From a quality-control perspective, cylinder-bore condition is better assessed by combining dimensional and surface measurements rather than relying on the bore diameter alone. Diameter, ovality, roundness, taper, and cylindricity describe different aspects of bore geometry, while roughness and cross-hatch inspection provide information on surface condition. Blow-by and oil consumption can complement these measurements at the engine

level, but should remain supporting indicators because they are also influenced by other engine-system factors.

These measurements were collected by separate teams as part of the production workflow. Routine weekly quality inspection covers the bore geometry, surface roughness, cross-hatch condition, and bore position, whereas the dynamometer team records the blow-by and oil consumption. In this study, the records were linked through the production and assembly history of each selected engine, allowing the initial inspection results to be considered along with the post-test bore measurements and engine-level responses. This integration uses existing measurement equipment and procedures instead of introducing a new inspection system.

Although individual measurements are already part of routine inspection and engine testing, their integration into a single pre-test and post-test assessment has so far been demonstrated only for the six engines in this study. The approach has not yet been adopted as a standard procedure across the production line. Wider application would require evaluation with a larger engine population under additional operating conditions. The present study therefore demonstrates the feasibility of linking existing measurements but does not establish plant-wide implementation or universal applicability.

4.9. Measurement and Experimental Limitations

Several limitations should be considered when interpreting the present findings. The study included six new production engines, with three in each group. However, the engines originated from different production dates and batches. With this small sample, engine-to-engine variability cannot be separated from potential batch-related effects. Therefore, the ICE–HEV comparison should be interpreted as descriptive for the tested engines and not generalised to the wider engine population.

Second, the geometry and surface measurements were obtained at the cylinder level, whereas blow-by and oil consumption were measured at the engine level. This difference in the experimental hierarchy means that cylinder measurements should not be treated as independent engine replicates.

Third, surface roughness was measured using one trace at each predefined location rather than repeated traces. Therefore, local variations in honing texture could not be separated from the measured changes, and the repeatability of the roughness measurements was not quantified. The bore diameter was measured manually using a dial bore gauge, with three readings taken at each measurement point and averaged. However, no formal Gauge R&R study, independent inter-operator assessment, or comparison with digital bore-measurement equipment was conducted. Although the gauge had a valid calibration record, the uncertainty of the complete measurement procedure was not established. These limitations should be considered when interpreting small dimensional and surface changes.

In addition, direct material loss or wear-volume measurements were not performed. Consequently, the present study cannot quantitatively distinguish surface modification associated with running-in from localised material removal or progressive wear. The roughness and cross-hatch results should therefore be regarded as complementary surface-condition indicators rather than direct measurements of wear severity.

Fourth, oil and coolant temperatures were available as supporting test-control measurements; however, the small number of independent engines and controlled operating conditions did not support the treatment of these thermal values as separate explanatory variables. Therefore, they were used to confirm comparable test exposure rather than for the causal interpretation of ICE–HEV differences.

The single 6000 rpm and full-load conditions also limit the representation of the wider operating and duty cycle conditions experienced by ICE and HEV engines during service.

In particular, the continuous dynamometer condition did not reproduce the start–stop and variable duty cycle characteristics that are normally associated with HEV operation.

Finally, the M1–M2 comparison represents the net change between the two measurement states. The individual contributions of assembly induced distortion, residual stress, thermal exposure, and wear cannot be separated using the present experimental design. No engine-specific finite element model was developed in this study. The numerical studies discussed in Section 4.1 provide context for possible deformation mechanisms but do not validate the measurements obtained from the six engines. In addition, the cylinder head was removed during both measurement stages. The measured changes should therefore be interpreted as differences between the pre-test and post-test states, rather than as direct measurements of bore deformation under assembled, hot operating conditions.

These limitations do not undermine the value of the experimental comparison but define the strength of the conclusions that can be reasonably drawn. The current evidence supports the measured post-test changes and their associations with engine-level responses rather than isolated causal claims.

Future studies should include a larger number of independent engines, repeated roughness traces, a comparison with digital bore-measurement equipment, and formal measurement-system repeatability and reproducibility studies. Measurements taken before assembly, after assembly, after controlled thermal conditioning, and after dynamometer operation would help separate assembly related, thermal, stress-related, and operating effects. An engine-specific thermomechanical finite element model can also be developed using the relevant engine geometry, material properties, assembly conditions, and available operating data [41]. The model should then be validated against experimental measurements obtained under comparable conditions.

With a larger engine-level sample, a hierarchical linear mixed-effects model could be used to quantify the effects of engine group, measurement stage, and axial position while accounting for engine-to-engine and cylinder-to-cylinder variability. Engine group, measurement stage, axial position, and their relevant interactions could be specified as fixed effects, while engine and cylinder nested within engine could be specified as random intercepts. Where sufficient repeated measurements are available, random slopes for measurement stage or axial position could also be considered. This approach would preserve the nested engine–cylinder measurement hierarchy and account for the dependence of repeated measurements obtained from the same cylinder and engine.

5. Conclusions

Controlled dynamometer operation resulted in measurable changes in cylinder-bore geometry and surface condition in both engine groups. The ICE engines showed larger mean changes in bore diameter and ovality, whereas the HEV engines showed larger changes in roundness and cylindricity. Reductions in surface-roughness parameters were more pronounced in the ICE group, while the cross-hatch evaluations remained within the acceptance criteria for both groups. The mean blow-by and oil-consumption values were lower in the HEV group. These engine-level responses provide supporting information on sealing and oil-control behaviour but cannot be attributed directly to bore deformation.

The practical contribution of this study lies in linking routine inspection records with post-test bore measurements and engine-level dynamometer results through production and assembly traceability. This provides a basis for interpreting existing measurements together, although the integrated assessment has not yet been adopted as a standard procedure.

The findings are limited to six engines, comprising three ICE and three HEV engines, tested under the specified dynamometer conditions. The principal comparison was conducted at 6000 rpm and 100% torque. The observed differences should therefore be treated

as descriptive findings for the tested engines rather than generalised to the wider engine population or other operating conditions. In particular, the continuous dynamometer test did not reproduce the start–stop and variable duty-cycle characteristics of HEV operation. Further work should examine a larger engine population and additional operating conditions to evaluate the repeatability and broader applicability of the integrated assessment.

Author Contributions: Conceptualisation, M.A.S.A. and M.T.H.S.; methodology, M.A.S.A.; validation, M.T.H.S., J.L.T. and N.K.C.; formal analysis, M.A.S.A.; investigation, M.A.S.A.; resources, J.L.T. and N.K.C.; data curation, M.A.S.A.; writing—original draft preparation, M.A.S.A.; writing—review and editing, M.T.H.S., J.L.T. and N.K.C.; visualisation, M.A.S.A.; supervision, M.T.H.S.; project administration, M.T.H.S. All authors have read and agreed to the published version of the manuscript.

Funding: The authors are grateful for the financial support given by The Ministry of Higher Education Malaysia (MOHE) under the Higher Institution Centre of Excellence (HICOE2.0/5210004) at the Institute of Tropical Forestry and Forest Products.

Institutional Review Board Statement: Not applicable.

Informed Consent Statement: Not applicable.

Data Availability Statement: Data are available upon request from the corresponding author.

Acknowledgments: The authors also thank the Department of Aerospace Engineering, Faculty of Engineering, Universiti Putra Malaysia, and the Laboratory of Biocomposite Technology, Institute of Tropical Forestry and Forest Products (INTROP), Universiti Putra Malaysia (HICOE) for their close collaboration in this study.

Conflicts of Interest: The authors declare no conflicts of interest.

References

1. Delprete, C.; Razavykia, A. Piston Ring–Liner Lubrication and Tribological Performance Evaluation: A Review. *Proc. Inst. Mech. Eng. Part J J. Eng. Tribol.* **2018**, *232*, 193–209. [CrossRef]
2. Bi, Y.; Xu, Y.; Liu, S.; Chen, S.; Shen, L.; Xu, Y. Cylinder Liner Deformation Characteristics Based on Fourier Transform and Impact on Ring Pack Sealing and Friction Power. *J. Braz. Soc. Mech. Sci. Eng.* **2023**, *45*, 242. [CrossRef]
3. Cheng, C.; Kharazmi, A.; Schock, H.; Wineland, R.; Brombolich, L. Three-Dimensional Piston Ring–Cylinder Bore Contact Modeling. *J. Eng. Gas Turbines Power* **2015**, *137*, 111505. [CrossRef]
4. Ali, S.H.R.; Bedewy, M.K.; Zahwi, S.Z. Dimensional Inspection of Overhauled Automotive Water-Cooled Diesel Engines. In Proceedings of the 9th International Conference on Production Engineering, Design and Control, Alexandria, Egypt, 10 February 2009; pp. 1–10.
5. Pawlus, P.; Reizer, R.; Wieczorowski, M. Analysis of Surface Texture of Plateau-Honed Cylinder Liner—A Review. *Precis. Eng.* **2021**, *72*, 807–822. [CrossRef]
6. Pawlus, P.; Koszela, W.; Reizer, R. Surface Texturing of Cylinder Liners: A Review. *Materials* **2022**, *15*, 8629. [CrossRef] [PubMed]
7. Gao, L.; Liu, S.; Xu, Z.; Li, B.; Cui, Y.; Meng, X. Tribo-Dynamic Modeling Method and Application to Three-Dimensional Flexible PRL System. *Int. J. Mech. Sci.* **2024**, *277*, 109446. [CrossRef]
8. Lü, Y.; Kang, J.; Zhao, X.; Zhang, Y.; Yang, X.; Chen, R.; Xing, Z. Effects of Different Surface Textures on Tribological Performances of the Cylinder Liner-Piston Ring: An Experimental Study. *Int. J. Engine Res.* **2024**, *25*, 545–556. [CrossRef]
9. Baby, A.K.; Rajendrakumar, P.K.; Lawrence K, D. Influence of Honing Angle on Tribological Behaviour of Cylinder Liner–Piston Ring Pair: Experimental Investigation. *Tribol. Int.* **2022**, *167*, 107355. [CrossRef]
10. Delprete, C.; Selmani, E.; Bisha, A. Gas Escape to Crankcase: Impact of System Parameters on Sealing Behavior of a Piston Cylinder Ring Pack. *Int. J. Energy Environ. Eng.* **2019**, *10*, 207–220. [CrossRef]
11. Zhong, X.; Tian, T. Oil Transport Simulation and Oil Consumption Prediction with a Physics-Based and Data-Driven Digital Twin Model for Internal Combustion Engines. *Lubricants* **2025**, *13*, 463. [CrossRef]
12. Liang, J.; Zhao, H.D.; Song, F.C. Development of a Laser-Based Measuring System for the Inner Geometrical Dimension of Cylinder Liner. *Results Opt.* **2020**, *1*, 100033. [CrossRef]
13. Ali, S.H.R.; Mohamed, H.H.; Bedewy, M.K. Identifying Cylinder Liner Wear Using Precise Coordinate Measurements. *Int. J. Precis. Eng. Manuf.* **2009**, *10*, 19–25. [CrossRef]

14. Walid, A.; Eifler, M. Common Practices and Methodologies in Scientific Functional Characterization of Surface Topography. *Metrology* **2025**, *5*, 33. [CrossRef]
15. Zhmud, B.; Chobany, D. Mastering the Art of Cylinder Bore Honing. *SAE Int. J. Adv. Curr. Pract. Mobil.* **2020**, *3*, 583–589. [CrossRef]
16. Ma, W.; Biboulet, N.; Lubrecht, A.A. Cross-Hatched Groove Influence on the Load Carrying Capacity of Parallel Surfaces with Random Roughness. *Tribol. Int.* **2021**, *153*, 106610. [CrossRef]
17. Reizer, R.; Pawlus, P.; Wieczorowski, M. Simulation of Plateau-Honed Cylinder Liner Surface Texture Creation Using Superimposition Approach. *Precis. Eng.* **2023**, *82*, 10–24. [CrossRef]
18. Podulka, P. Fast Fourier Transform Detection and Reduction of High-Frequency Errors from the Results of Surface Topography Profile Measurements of Honed Textures. *Eksploat. Niezawodn.–Maint. Reliab.* **2021**, *23*, 84–93. [CrossRef]
19. He, B.; Ding, S.; Wei, C.; Shi, Z. The Influence of the Choice of a Gaussian Filter on the Determination of Areal Surface Texture Parameters. *Instrum. Exp. Tech.* **2021**, *64*, 71–77. [CrossRef]
20. El Mansori, M.; Goeldel, B.; Sabri, L. Performance Impact of Honing Dynamics on Surface Finish of Precoated Cylinder Bores. *Surf. Coat. Technol.* **2013**, *215*, 334–339. [CrossRef]
21. Angermann, C.; Haltmeier, M.; Laubichler, C.; Jónsson, S.; Schwab, M.; Moravová, A.; Kiesling, C.; Kober, M.; Fimml, W. Surface Topography Characterization Using a Simple Optical Device and Artificial Neural Networks. *Eng. Appl. Artif. Intell.* **2023**, *123*, 106337. [CrossRef]
22. Eifler, M.; Brodmann, B. Phase-Space-Based Fusion of Angular and Height Data in Tactile and Optical Surface Texture Measurement for Tribological Analysis. *Measurement* **2026**, *266*, 120339. [CrossRef]
23. Hernández-Comas, B.; Maestre-Cambronel, D.; Pardo-García, C.; Fonseca-Vigoya, M.D.S.; Pabón-León, J. Influence of Compression Rings on the Dynamic Characteristics and Sealing Capacity of the Combustion Chamber in Diesel Engines. *Lubricants* **2021**, *9*, 25. [CrossRef]
24. Rossegger, B.; Eder, M.; Vareka, M.; Engelmayer, M.; Wimmer, A. A Novel Method for Lubrication Oil Consumption Measurement for Wholistic Tribological Assessments of Internal Combustion Engines. *Tribol. Int.* **2021**, *162*, 107141. [CrossRef]
25. Yang, Z.; Li, B.; Yu, T. Distortion Optimization of Engine Cylinder Liner Using Spectrum Characterization and Parametric Analysis. *Math. Probl. Eng.* **2016**, *2016*, 1–11. [CrossRef]
26. Bhosale, A.J.; Bansode, K.B.; Kakde, R.P.; Dhepe, V.Y.; Patil, S.D. Cylinder Bore Deformation Finite Element Analysis Methodology for Inline Engines and Parametric Optimization. *Int. J. Recent Technol. Eng.* **2020**, *8*, 934–939. [CrossRef]
27. Bao, Y.; Lei, J.; Li, W.; Deng, W.; Deng, X.; Xu, Y.; Song, G.; Dai, G. Research on Thermal Deformation of Cylinder Bore with Orthogonal Experiment Method of Aluminum Alloy Cylinder Block in Diesel Engine. *Appl. Therm. Eng.* **2024**, *245*, 122772. [CrossRef]
28. Li, W.; Lei, J.; Bao, Y.; Deng, W.; Jia, D.; Wang, P.; Xu, Y. Research on Cylinder Bore Deformation in Aluminum Alloy Cylinder Block of Diesel Engine under Bolt Preload. *Eng. Sci. Technol. Int. J.* **2026**, *76*, 102317. [CrossRef]
29. Rao, X.; Sheng, C.; Guo, Z.; Zhang, X.; Yin, H.; Xu, C.; Yuan, C. Effects of Textured Cylinder Liner Piston Ring on Performances of Diesel Engine under Hot Engine Tests. *Renew. Sustain. Energy Rev.* **2021**, *146*, 111193. [CrossRef]
30. Kim, E.-S.; Lee, Y.-Z. Investigation of the Effects of Uneven Plateau Grinding on Friction, Wear Rate, and Localized Surface Damage on Internal Combustion Engine Cylinder Liners. *Int. J. Automot. Technol.* **2021**, *22*, 561–567. [CrossRef]
31. Nagai, S.; Yoshida, I.; Oshiro, K.; Sakakibara, R. Acceleration of Surface Roughness Evaluation Using RANSAC and Least Squares Method for Running-in Wear Process Analysis of Plateau Surface. *Measurement* **2022**, *203*, 111912. [CrossRef]
32. Nowak, N.; Scheiber, K.; Pfeil, J.; Meyer, J.; Dittler, A.; Koch, T.; Kasper, G. Sampling and Conditioning of Engine Blow-by Aerosols for Representative Measurements by Optical Particle Counters. *J. Aerosol Sci.* **2020**, *148*, 105612. [CrossRef]
33. Wang, P.; Bi, Y.; Xie, G.; Lei, J.; Peng, Y. Thermo-Mechanical Deformation Control of a Cylinder Liner Using Segmented Pre-Compensation Design. *Int. J. Engine Res.* **2026**, *in press*. [CrossRef]
34. Miao, C.; Guo, Z.; Yuan, C. Tribological Behavior of Co-Textured Cylinder Liner-Piston Ring during Running-In. *Friction* **2022**, *10*, 878–890. [CrossRef]
35. Kang, J.; Lu, Y.; Yang, X.; Zhao, X.; Zhang, Y.; Xing, Z. Modeling and Experimental Investigation of Wear and Roughness for Honed Cylinder Liner during Running-in Process. *Tribol. Int.* **2022**, *171*, 107531. [CrossRef]
36. Wu, D.; Liang, X.; Wen, X.; Meng, Z.; Yu, Z.; He, Y.; Dai, P.; Yu, Y.; Li, N. Experimental Study of Diesel Engine Deposits on Failure of Honed Cylinder Liner Surface Texture. *Eng. Fail. Anal.* **2025**, *174*, 109476. [CrossRef]
37. Li, M.; Tian, T. Effect of Blowby on the Leakage of the Three-Piece Oil Control Ring and Subsequent Oil Transport in Upper Ring-Pack Regions in Internal Combustion Engines. *Lubricants* **2022**, *10*, 250. [CrossRef]
38. Liu, X.; Cao, X.; Ma, X.; Li, M. Surface Characterization of Cylinder Liner–Piston Ring Friction Pairs Under Different Temperature and Load by Power Spectral Density Method. *Lubricants* **2025**, *13*, 237. [CrossRef]
39. Ge, C.; Zhang, B.; Xu, X.; Lyu, X.; Ma, X.; Li, T.; Lu, X.; Liu, Z. Tribofilm Distribution and Tribological Analysis of Piston Ring-Cylinder Liner Interfaces under Realistic Engine Conditions. *Tribol. Int.* **2025**, *201*, 110250. [CrossRef]

40. Puoza, J.C.; Amedorme, S.K.; Musah, A.; Ibrahim, A.; Kuusana, Y. Evolution of Surface Engineering Technology in Cylinder Liner-Piston Ring System of Internal Combustion Engines. *J. Eng.* **2025**, *2025*, e70152. [CrossRef]
41. Tai, J.L. Finite Element Method for Sustainable Structural Integrity of Multi-Bolted Flanges: A Review of Optimized Design and Green Maintenance Strategies. *J. Kejuruter.* **2026**, *38*, 3271–3286. [CrossRef] [PubMed]

Disclaimer/Publisher's Note: The statements, opinions and data contained in all publications are solely those of the individual author(s) and contributor(s) and not of MDPI and/or the editor(s). MDPI and/or the editor(s) disclaim responsibility for any injury to people or property resulting from any ideas, methods, instructions or products referred to in the content.